UNIVERSITY OF CALIFORNIA SAN DIEGO

Mechanisms of Post-Transcriptional Regulation in S. cerevisiae

A dissertation submitted in partial satisfaction of the
requirements for the degree Doctor of Philosophy

in

Chemistry

by

Vince Harjono

Committee in charge:

Professor Brian Zid, Chair
Professor Daniel Donoghue
Professor Judy Kim
Professor Jens Lykke-Andersen
Professor Ulrich Muller

2022

The dissertation of Vince Harjono is approved, and it is acceptable in quality and form for publication on microfilm and electronically.

University of California San Diego

2022

DEDICATION

This work is dedicated to my family who have always strove to support me and give me a better life. To my loving parents, Elizabeth H. Junus and Budi Harjono. To my cooler and supportive brother, Calvin Harjono. To my grandmother who always calls me at inopportune times, Erna Junus. And finally, to the rest of my large, unique, and supportive family. I would not be where I am today without your support.

TABLE OF CONTENTS

LIST OF ABBREVIATIONS

1,10-PNT	1,10-Phenanthroline
AA	Amino Acids
ATC	Anhydrotetracycline
cDNA	Complementary DNA
CDS	Coding Sequence
DNA	Deoxyribonucleic Acid
miRFP	Monomeric Infrared Fluorescent Protein
mRNA	Messenger RNA
mRNP	Messenger Ribonucleoprotein
NGD	No-Go Decay
nLuc	Nanoluciferase
ORF	Open Reading Frame
PBs	Processing Body
PCR	Polymerase Chain Reaction
qPCR	Quantitative Polymerase Chain Reaction
RLU	Relative Light Unit
RNA	Ribonucleic Acid
RQC	Ribosome Quality Control
RT	Reverse Transcription
SG	Stress Granule
TET	Tetracycline
tRNA	Transfer RNA

UTR	Untranslated Region
WT	Wild Type
YFP	Yellow Fluorescent Protein

LIST OF FIGURES

LIST OF TABLES

ACKNOWLEDGMENTS

I scarcely believe that I am reaching the end of the long journey that is grad school and by extension, likely the end of my academic scientific training. One reason I applied to grad school is because I felt that my undergraduate education in biology at UC Davis, while a distinguished program, was incomplete - there remained so much to learn. As I write this over a decade since I began my formal education in the sciences, I still feel that there remains so much to learn and I am excited to see what comes next. Looking back through my academic career, I am humbled by how fortunate I have been to have met such intelligent, personable, and kind individuals, many of whom are among my closest and lifelong friends. I could not ask for a better group of people to have shared my graduate school experience with. Here, I acknowledge the amazing people and pets that have lent me their support during my career in grad school and without whom I would not have had such an enjoyable and fulfilling experience. By no means does this constitute an exhaustive list and I have nothing but gratitude all those who have made my time at UCSD special.

First and foremost, I would like to thank my thesis advisor Brian for his constant support and guidance. I am doubtful that any other PI would provide the same level of trust, flexibility, and unwavering optimism towards the frequent setbacks, stalling projects, and negative data. I find it plausible that this man was descended from Ghandi himself as I have rarely seen such patience. I am truly grateful to have had the many opportunities in the Zid lab to take risks, make mistakes, learn, and improve myself as both a person and scientist. I believe Brian’s charisma and love for science coalesced

into a lab group that was friendly and supportive and whose dynamic was the envy of many. Throughout the highs and lows of research, you had my back. Thank you Brian, truly, for taking me on as a student.

I would like to thank my committee members for their advice and guidance throughout my grad school education. I wish that I had utilized you all more as a valuable resource to shape my thesis direction and to ask for advice but I remain grateful for the assistance and supervision you have provided me over the years. Thank you Uli, Judy, Dan, and Jens (Dr. Ulrich F. Muller, Dr. Judy Kim, Dr. Daniel Donoghue, & Dr. Jens Lykke-Andersen).

I would like to thank my family, all of whom don't understand what I do but nonetheless are proud of me and supportive to a fault. To my mom Elizabeth and dad Budi, both of you have made it your life's work to care for Calvin and I. To Calvin, my wildly successful little brother who still regularly calls me to chat about life and to share advice. To my grandma Erna, who to this day thinks I am a physician. To my crazy aunts, all of which have made my life colorful and interesting. To Alex, my older cousin who introduces me to games and hobbies and without whom I would have likely finished a month or two sooner. And to the rest of my unique, supportive, and loving family. Thank you for all your support.

To my wonderful friends who have my time in grad school memorable and have supported me through the ups and downs, I thank you deeply. To Anna, one of the first close and lifelong friends I developed in grad school and who I shared lunch with nearly every day and introduced me to all the amazing people in the biology program. To Hema, an intelligent, ambitious, and kind person who is one of my closest friends and

fervent supporters. To Ximena, a constant source of conversation, satire, snark, entertainment, and bathroom humor. To the remainder of the Zid lab and in particular the group of undergrads known as the Girlbosses. To my friends in the Muller, Toor, Joseph, and McHugh RNA labs especially Josh, Kevin, and Arvin. To my friends in the biology department, consulting club, and all others I have met through UCSD. And of course, I cannot forget the pets that are a steady source of entertainment, comfort, and love. To the amazing dogs, cats, and lizard: Wally, Kique, Adora, the Berts, Waffles, Waffle, Bruce, Blueberry, Pepper, and Stevie, Sasha, Rainey, Charlie, and Muzzy.

Thank you to Janice, my partner. You have been so supportive and loving since I've known you and you have made my last year and a half of grad school more special than I can describe. Thank you for being by my side and continuing to support my quirky antics, horrible puns, and obsession with my dog.

Lastly, I would like to thank Ellie, my golden retriever. I can't overstate how much you've been a source of emotional comfort and joy to me and others. I sincerely believe that you have made me a better person and I thank you for helping me through the roughest of times in grad school. You will always be my lovable, goofy, food-driven, and faithful companion and I will always be your person.

Chapter 2, in full, is currently being prepared for submission for publication of the material: Harjono, V, Hou, W, Harvey, AT, Subramaniam, AR, and Zid, BM. Quantification of elongation stalls and impact on gene expression in yeast. The dissertation author is the primary author of this material.

Chapter 3 consists of both published and unpublished material. Section 3.2, in part, is a partial reprint of the following published manuscript: Chen, YS, Tracy, S,

Harjono, V, Xu, F, Moresco, JJ, Yates, JR, and Zid, BM. Rvb1/Rvb2 proteins couple transcription and translation during glucose starvation. *bioRxiv* (2021). https://doi.org/10.1101/2021.10.17.464753. The dissertation author is the third author of this paper. Section 3.3 consists of unpublished material. The dissertation author is the primary author of this material.

VITA

EDUCATION

2022 Doctor of Philosophy in Chemistry, University of California San Diego

2017 Master of Science in Chemistry, University of California San Diego

2015 Bachelor of Science in Biotechnology, University of California Davis

RESEARCH EXPERIENCE

University of California, San Diego 2015-2022

Graduate Student Researcher in the laboratory of Dr. Brian M. Zid

Department of Chemistry & Biochemistry

Investigation into post-transcriptional regulatory mechanisms in yeast

University of California, Davis 2013-2015

Undergraduate Researcher in the laboratory of Dr. Marie Jasieniuk

Department of Agricultural Sciences

Study of the spread of herbicide resistance in ryegrass populations in California

PUBLICATIONS

Harjono, V., Hou, W., Harvey, A. T., Subramaniam, A. R., & Zid, B. M. (2022). Quantification of codon-associated stalling effects on elongation. Manuscript in preparation for submission.

Chen, Y. S., Tracy, S., **Harjono, V.,** Xu, F., Moresco, J. J., Yates, J. R., & Zid, B. M. (2021). Rvb1/Rvb2 proteins couple transcription and translation during glucose starvation. *bioRxiv*.

Loureiro, M.E., Zorzetto-Fernandes, A.L., Radoshitzky, S., Chi, X., Dallari, S., Marooki, N., Lèger, P., Foscaldi, S., **Harjono, V.,** Sharma, S., Zid, B.M., López, N., Carlos de la Torre, J., Bavari, S. and Zúñiga, E. (2018). DDX3 suppresses type I interferons and favors viral replication during Arenavirus infection. *PLoS pathogens*, *14*(7), p.e1007125

ABSTRACT OF THE DISSERTATION

Mechanisms of Post-Transcriptional Regulation in S. Cerevisiae

by

Vince Harjono

Doctor of Philosophy in Chemistry

University of California San Diego, 2022

Professor Brian M. Zid, Chair

Post-transcriptional regulation represents a powerful and versatile mechanism to fine-tune gene expression to meet cellular and environmental demands. One important aspect of post-transcriptional regulation involves regulation of protein translation, the process of building proteins from a messenger RNA. In this dissertation, I use biochemical and molecular biology techniques to study how translation is mechanistically regulated by both mRNA and protein factors. In chapter 2, I discuss the development of a quantitative method in eukaryotes to measure ribosomal stalls of *cis*-mRNA factors on protein elongation. We find that different distributions of nonoptimal codons trigger different surveillance and rescue pathways despite similar levels of elongation delay. In chapter 3, I explore the relationship between translatability and mRNA localization during glucose starvation and investigate potential factors that influence this relationship. We find that a complex made from Rvb1 and Rvb2 is involved in promoter-directed cytoplasmic fate in a subset of stress response genes in glucose starvation. Furthermore, we use carefully designed reporters to interrogate how translatability determines cytoplasmic localization and find that active translation is linked to exclusion from stress-induced cytoplasmic granules. Finally in chapter 4, I discuss improvements on the method we have developed, possible future directions for the work described in this dissertation, and my concluding remarks.

CHAPTER 1: Introduction

1.1 Protein Synthesis and Post-Transcriptional Regulation

Cellular survival and proliferation depends on careful regulation of protein synthesis, which represents the most energy-intensive process in the cell, consuming over 70% of cellular ATP levels (Stouthamer 1973, Buttgereit and Brand 1995, Wieser and Krumschnabel 2001). This crucial task of maintaining cellular homeostasis is represented by a complicated coordination of countless interacting biological factors both spatially and temporally. Since 1838 when proteins were discovered and the word 'protein' was coined by Jöns Jakob Berzelius, researchers have attempted to identify and characterize the factors involved in protein synthesis (Hartley 1951). As proteins are the final product of most gene expression, protein synthesis involves multiple layers of regulation both at the DNA and RNA stages. While we have learned much about the basic mechanisms since then, many factors and how they interact with other factors remains undiscovered.

Post-transcriptional regulation affects mRNA before, during, and after protein translation has occurred. Mutations in post-transcriptional regulatory factors, especially RNA-binding proteins, have been linked to proliferation of cancer in humans and contributes to a general misregulation of gene expression (Audic and Hartley 2004, Corbett 2018). Both a function of mRNA *cis*-elements and *trans*-factors, post-transcriptional regulation of gene expression includes varying mRNA abundance through balancing transcription and decay, modifications to mRNA, and elements that affect translational efficiency, such as regulatory sequences, sequence composition, and tRNA abundance (Schaefke et al. 2018, Obernosterer et al. 2006, Furlan et al.

2021, Corbett 2018, Kim and Lee 2012, Lawless et al. 2009, Beyer et al. 2004, Kos-Braus and Koš 2017, McCarthy 1998). Furthermore, these factors can be spatially regulated, such as in mRNA localization and subcellular compartmentalization, and temporally regulated, such as in rapid induction of transcription or degradation of transcripts in response to specific stimuli (Pakos-Zebrucka et al. 2016, Buxbaum et al. 2015). It is through the complex orchestration of all these factors that cells can finely tune their proteome to meet cellular demands and adapt to changing environmental stimuli. In this chapter, I will introduce and describe a few of the mechanisms of post-transcriptional regulation, their factors, and how they interact and combine to exert effects on protein synthesis.

1.2 Codons, Codon Optimality, and Implications on mRNA Stability and Translation

During translation elongation, amino acids are added to a growing peptide chain specified by the sequence of codons present in the mRNA transcript. Codons, three base pair combinations of the canonical four nucleotides in RNA, are decoded by ribosome in which a tRNA bearing a corresponding anti-codon will bring a specific amino acid to form a peptide bond onto the nascent protein chain. The amino acid code is redundant; with 61 unique codons specifying 20 different amino acids, each amino acid is specified by between one and six codons. With the advent of genome sequencing, genomes have been found to contain unequal frequencies of synonymous codons and these codon biases are unique across species (Grantham et al. 1980, Bennetzen and Hall 1982, Guoy and Gautier 1982). Furthermore, differentiating factors

between codons such as GC content, speed of peptide bond formation, and tRNA availability contribute to a metric known as normalized translational efficiency (nTE) (Pechmann and Frydman 2013). The nTE scale assigns a score to each codon from 0 to 1 that represents the translational efficiency of the codon, incorporating the previous tRNA adaptation index (tAI) and tRNA supply and demand based on charged tRNA abundance and transcriptomic demand (Reis et al. 2004). Based on the nTE scale, codons are considered “optimal” if their relative tRNA availability is higher than their demand whereas they are considered “nonoptimal” if their relative tRNA availability is less than their demand.

Comparisons of transcripts enriched in either optimal or nonoptimal codons have revealed correlations between codon optimality and other regulatory metrics. For instance, codon optimality has been linked to mRNA half-life. Genome-wide RNA decay comparisons between stable and unstable mRNAs revealed that stable mRNAs are enriched in optimal codons whereas unstable mRNAs are enriched in nonoptimal codons (Presnyak et al. 2015). Furthermore, substitution of optimal codons to synonymous nonoptimal codons led to mRNA destabilization. It has been thought that the DEAD-Box protein Dhh1p mediates this interaction by sensing transcripts enriched in nonoptimal codons and signaling them for mRNA decay (Radhakrishnan 2016, Harigaya and Parker 2016, Hanson and Coller 2018). In the context of protein expression, Dhh1 links nonoptimal codons to lower protein expression through a reduction in mRNA levels.

Codon optimality plays a further role in regulating the rate of ribosome translocation during elongation. Codon identity has long been shown to affect

translation elongation rate and newer techniques such as ribosome profiling have supported this finding though genome-wide ribosome occupancy measurements (Sørensen & Pedersen 1991, Ingolia 2014, Ingolia et al. 2009, Hussman et al. 2015, Gardin et al. 2014, Weinberg et al. 2016, Saikia et al. 2016). In general, there is a correlation between optimal codons having faster elongation rates as compared to nonoptimal codons. The difference in elongation rates is primarily due to two factors: (1) charged tRNA availability as ribosomes will on average wait longer to find a rare cognate tRNA as compared to a commonly available tRNA and (2) the time ribosomes require to sample tRNAs to find a cognate tRNA, especially if near-cognate tRNAs are more abundant (Chu et al. 2011, Koutmou et al. 2015). This reduction of elongation rate ultimately leads to a reduction of protein expression as fewer proteins are produced in a given time period, especially when considering the lower half-lives of nonoptimal mRNAs. Indeed, the nonoptimal rare arginine codon CGA has been shown to strongly inhibit protein expression and reduce translation elongation rate (Letzring et al. 2010, Kisly et al. 2021). It has been shown that varying the locations of optimal and nonoptimal codons has a functional role in co-translational protein folding (Thanaraj and Argos 1996, Yu et al. 2015, Xu et al. 2021, Collart and Weiss 2020). Experiments in *E.* coli have shown that substitution of rare codons for synonymous optimal codons leads to higher protein expression but also higher protein misfolding (Komar et al. 1999, Zhang et al. 2009). Furthermore, other experiments have shown that codon pairs and mRNA secondary structure have also been implicated in proper protein folding though modulation of elongation speed (Gamble et al. 2016, Yang et al. 2014). These studies provide evidence that regulation of elongation speed is crucial for proper cellular

function and one method cells employ is to utilize a combination of optimal and nonoptimal codons.

1.3 Ribosome Collisions and the RQC and NGD Surveillance Pathways

Many factors have been discovered that impede ribosome movement and slow down elongation speed. In the previous section, we examine evidence on how ribosomes will modulate elongation speed to promote protein folding through inclusion of slowing factors, including nonoptimal codons or RNA secondary structure. Mechanistically, ribosomes in eukaryotes will continue translocating across the mRNA at an average rate of 3-10 amino acids per second until it reaches an impediment where it will pause for an extended duration before it is able to continue forward, such as in the case of waiting for a rare cognate tRNA (Karpinets et al. 2006, Riba et al. 2019). As multiple ribosomes are often concurrently translating on a single mRNA, this ribosome pause may lead to an upstream translating ribosome reaching the paused ribosome, resulting in a ribosome collision and formation of a di-some structure. Genome-wide transcriptomic analysis of ribosome collisions through ribosome profiling have shown that upwards of 10% of all translating ribosomes are engaged in the di-some state, highlighting the prevalence of these ribosome collisions (Han et al. 2020, Arpat et al. 2020, Zhao et al. 2021). These ribosome collisions are not inherently detrimental; a recent paper looking into ribosome clearance times after encountering a stall showed that ribosomes are able to continue translocating after a collision has occurred (Goldman et al. 2021). However, cells must maintain careful surveillance of protein translation to detect collision events that may be detrimental to cellular survival.

Certain collision events require an active role in rescuing ribosomes to preserve protein fidelity and mitigate wasted resources. Deficiencies in protein fidelity may lead to deleterious molecules, which has been linked to neurological disease and proteotoxicity (Kapur and Ackerman 2008, Chu et al. 2009, Choe et al. 2016, Nedialkova and Leidel 2015, Yonashiro et al. 2016). Extended ribosome stalls may be caused by mRNA cis-factors, such as a premature poly-A tail, truncated mRNA undergoing decay, higher order mRNA structures, and nascent peptide interactions with the ribosome exit tunnel or by trans-factors, such as tRNA deficiencies, nutrient starvation, or cellular stress (Doma and Parker 2006, Letzring et al. 2013, Simms et al. 2014, Gamble et al. 2016, Collart and Weiss 2020, Yip and Shao 2021, Goldman et al. 2021, Meydan and Guydosh 2020, Han et al. 2020, Chandrasekaran et al. 2019). In these situations, extended stalls may lead to a compounding of ribosome collisions into di-somes, tri-somes, and higher order ribosome structures as translating ribosomes will continue to collide with stalled ribosomes. As translation termination in eukaryotes requires the presence of a stop codon in the ribosomal A-site, these stalled ribosomes are unable to be disassembled by canonical elongation release factors (Hellen 2018, Dever and Green 2012, Mitkevich et al. 2006, Jackson et al. 2012). Rescue pathways must then be initiated to disassemble and recycle these stalled ribosomes and to degrade the faulty transcript and nascent peptide.

The cell must distinguish between the far more prevalent benign ribosome collision events and the less frequent situations where ribosome rescue is necessary. Translation has been shown to be necessary to detect defects in mRNA, suggesting that surveillance mechanisms screen translation to determine mRNA integrity (van Hoof

& Wagner 2011, Shoemaker and Green 2012). The ribosome quality control (RQC) pathway is activated by a E3 ubiquitin ligase called Hel2 (yeast) or ZNF598 (mammals) which detects collided ribosomes through a specific ribosome-ribosome interface formed by di-some collisions and signals them for rescue (Ikeuchi et al. 2019, Pechmann et al. 2013, Joazeiro 2019, Brandman and Hegde 2016, Meydan and Guydosh 2020). Hel2 ubiquitinates the small subunit ribosomal protein uS10 which recruits the ribosome-associated quality control (RQC)-triggering (RQT) complex. The RQT complex, consisting of Slh1, Cue3, and Asc1, dissociates the ubiquitinated ribosomes into small and large subunits (Yip and Shao 2021, Matsuo et al. 2017, Sitron et al. 2017, Hashimoto et al. 2020, Juszkiewicz et al. 2020). Nascent peptides from stalled ribosomes are then degraded through the interactions of Rqc2 (NEMF in mammals), which prevents ribosomal subunit reassociation and recruits Ltn1 (Listerin in mammals) to polyubiquitinate nascent proteins for proteosomal degradation (Joazeiro 2019, Inada 2020, Brandman and Hegde 2016, Brandman 2012, Shen et al. 2015, Shao et al. 2015, Bengtson and Joazeiro 2010, Collart and Weiss 2019). Once the leading collided ribosomes are disassembled, trailing ribosomes may continue to elongate.

Concurrent with the activation of the RQC pathway, the transcript may be degraded through the No-Go Decay (NGD) pathway, which targets mRNAs containing stalled ribosomes. (Ikeuchi et al. 2019, Matsuda et al. 2014, Joazeiro 2017). During an extended stall, the ribosomal A-site remains empty allowing for a ternary complex comprised of Dom34 (Pelota in mammals), Hbs1, and GTP to bind and disassemble the ribosome (Pisareva et al. 2011, Shoemaker et al. 2010, Shoemaker and Green 2010,

Harigaya and Parker 2010, Simms et al. 2017). The endonuclease Cue2 (N4BP2 in mammals) is then recruited which cleaves the aberrant mRNA based on the density of ribosomal collisions and the remaining fragments are rapidly degraded by the cytoplasmic exosome and the exonucleases Xrn1 and Ski7 (Simms et al. 2017, Harigaya and Parker 2010, D'Orazio et al. 2019, Powers et al. 2020, Buskirk and Green 2017, Navickas 2020). Activation of the NGD pathway has been shown to require Hel2-mediated ribosomal ubiquitination, suggesting that both ribosome collision and the subsequent empty A-site are required for NGD activation (Garzia et al. 2017, Juszkiewicz and Hegde 2017).

Based on current understanding of ribosomal stalls, ribosome dissociation and rescue can occur through two separate, though concurrent and co-activated, pathways. Upon an extended ribosomal stall, trailing ribosomes may collide with the leading ribosome, resulting in a collision which recruits Hel2. Hel2 ubiquitinates the small ribosomal subunit which activates both the RQC and NGD pathways. In the RQC pathway, the RQT complex is recruited to dissociate the ribosomal subunits and Rqc1 and Ltn1 are recruited to degrade the nascent peptide chain. In the NGD pathway, the Dom34/Hbs1/GTP ternary complex is recruited to the empty ribosomal A-site to dissociate the ribosome and Cue2, the exosome, Xrn1, and Ski7 are recruited to degrade the mRNA transcript. While both these pathways work in tandem to maintain protein fidelity and promote ribosome recycling, the factors that contribute to the activation and overall impact of these pathways remains unclear. For example, while we understand that Hel2-mediated ribosomal ubiquitination is necessary for the activation of these pathways, the number of ubiquitinated or collided ribosomes, the duration of

the stall necessary to evoke a cellular response, and other contributing factors remain a subject of study and may differ between the two pathways. Furthermore, the degree to which these pathways exert their effects on ribosome dissociation, mRNA decay, and peptide degradation, may be fine-tuned depending on the severity of conditions during their activation and may also differ.

1.4 mRNA Localization

Partitioning of mRNA molecules to specific locations in the cell allows for local or compartmentalized regulation of gene expression and has been found to be involved in crucial cellular processes including development, determination of cell fate, cell motility, and membrane anchoring of proteins (Buxbaum et al. 2015, Kloc et al. 2002, Jansen 2001, Martin and Ephrussi 2009). RNA binding proteins (RBPs) account for a large majority of the localization effects of mRNA, including transport, protection, and anchoring while cis-elements in the mRNA direct where the messenger ribonucleoprotein (mRNP) complex localizes (Jambhekar and DeRisi 2007, Shahbabian and Chartrand 2012, Patel et al. 2012). A few notable examples of mRNA localization include nanos mRNA localization to the posterior side of the *D. melanogaster* oocyte to create a protein gradient crucial for proper development, asymmetric localization of Ash1 mRNA during budding in *S. cerevisiae* to switch mating types, and the formation of neuronal transport granules in neurons containing β-actin mRNA which are localized to the dendrites such that translation of actin will result in synaptic grown in response to synaptic activity (Buxbaum et al. 2015, Forrest and Gavis 2003, Gavis and Lehmann 1992, Long et al. 1997, Garner et al. 1988, Lécuyer et al. 2007, Cajigas et al. 2012,

Eliscovich et al. 2013, Zaessinger et al. 2006, Jain and Gavis 2008, Becalska et al. 2011, Böhl et al. 2000, Deng al. 2008, Bobola et al. 1996, Gonzalez et al. 1999). In these instances, mRNAs are often translationally repressed in transit to prevent to spatially regulate protein production and prevent unwanted translation (Besse and Ephrussi 2008, Abaza and Gebauer 2008). However, active translation may also play a role in localization of mRNAs.

Localization signals do not only exist in the cis-sequence of the mRNA, but also in the nascent peptide produced during translation. One well studied localization signal in eukaryotes is the signal peptide, a short peptide sequence usually found at the N-terminus of a protein that is recognized by the signal recognition particle (SRP) (Ogg and Walter 1995, Kapp et al. 2009, Walter et al. 1981). The SRP is a RNP complex that binds to the signal sequence, leading to an elongation stall, and localizes to a translocon on the endoplasmic reticulum (ER) surface, allowing the nascent peptide to be inserted into the translocon channel such that the nascent peptide is directed into the ER (Tisdale and Pellizzoni 2017, Walter and Blobel 1983, Gilmore et al. 1982, Lutcke 1995, Luirink and Sinning 2004, Walter et al. 1981). While elongation arrest has shown not to be necessary for translocation of the SRP complex to a translocon, it provides additional time for the SRP complex to recognize, bind, and localize the mRNA and nascent signal peptide to the ER (Siegel and Walter 1985, Siegel and Walter 1988, Mason et al. 2000). This mechanism of elongation stalling has been seen in other signaling peptides such as the mitochondrial targeting sequence (MTS) in the gene ATP3, which contains a downstream stretch of polyproline residues that are important for increased localization to the mitochondrial surface (Tsuboi et al. 2020, Tsuboi et al.

2020). mRNA localization represents a powerful, conserved mechanism to fine-tune gene expression spatially.

1.5 Stress Response and mRNP Granules

Cells must rapidly adapt to changing environmental conditions to maintain cellular survival and homeostasis. Certain detrimental environmental conditions threaten cellular survival, including nutrient deprivation and stressors such as oxidative stress, osmotic stress, and severe DNA damage. As a cellular stress response requires the production of stress mitigating proteins, both the cellular proteome and transcriptome must quickly shift to prioritize cellular survival and recovery. This is accomplished through the activation of the integrated stress response (ISR) pathway, which senses cellular stress signals and initiates a signaling cascade (Pakos-Zebrucka et al. 2016). The core of the ISR pathway is eukaryotic translation initiation factor 2 (eIF2α), which is necessary for canonical cap-dependent translation initiation. Depending on the nature of the stress signal, the eIF2α kinases GCN2, PKR, HRI, or PERK will be activated and phosphorylate the alpha subunit of eIF2α on serine 51, preventing the formation of a viable ternary complex required for canonical cap-dependent translation initiation. Phosphorylation of eIF2α in the ternary complex, composed of eIF2α, the initiator methionine, and GTP, prevents exchange of GDP for GTP. This results in a global attenuation of translation, freeing up translation machinery for induced stress response genes. However, cells must maintain mechanisms for these stress response genes to selectively bypass translational shutdown.

Concurrent with the onset of stress in eukaryotes are the formation of stress granules (SGs) and processing bodies (PBs), two types of liquid-liquid phase-separated membrane-less mRNP granules (Buchan & Parker 2009, Khong et al. 2017, Teixeira et al. 2005, Jain et al. 2016, Guzikowski et al. 2019, Protter & Parker 2016, Corbet and Parker 2019, Van Treek and Parker 2019, Chernov et al. 2009). These large complexes, composed primarily of RBPs and non-translating mRNAs, are nucleated through RNA-RNA, RNA-protein, and protein-protein interactions (Begovich and Wilhelm 2020). The current model of mRNA localization into these granules stipulates that mRNAs are prevented from forming RNA-RNA interactions through the steric hindrance of ribosomes during elongation (Teixeira et al. 2005, Buchan et al. 2010, Guzikowski et al. 2019, Lin et al. 2015, Protter and Parker 2016, Van Treeck et al. 2018, Protter et al. 2018, Van Treeck and Parker 2018, Matheny et al. 2019, Wheeler et al. 2016). Once translation is attenuated through phosphorylation of eIF2α, initiation will be blocked. Ribosomes currently bound to transcripts will continue to elongate and eventually run off, resulting in exposed transcripts that are open to RNA-RNA interactions. Transcripts devoid of ribosomes will then aggregate with other RNA-binding proteins to nucleate these mRNP granules. Based on this model, mRNAs that can bypass the global shutdown of initiation and continue translating are more likely to be excluded from mRNP aggregation. Indeed, proteomic and transcriptomic analysis of SGs reveal that these are enriched in proteins containing intrinsically disordered regions (IDRs) and that contained mRNAs tend to be longer and poorly translated, both of which are more prone to aggregation (Jain et al. 2016, Khong et al. 2017, Matheny et al. 2019, Molliex et al. 2015).

Promoter sequences have been shown to direct cytoplasmic localization and translatability of genes during glucose starvation (Zid and O'Shea 2014). During glucose starvation, up to 10% of the pre-existing bulk mRNAs are sequestered into mRNP granules (Van Treeck et al. 2018, Khong et al. 2017). Meanwhile, certain classes of stress response genes such as heat shock proteins and alternative glucose metabolism genes are transcriptionally induced. However, heat shock proteins are translationally active and excluded from mRNP granules, appearing diffusely localized throughout the cytoplasm, while alternative glucose metabolism genes are sequestered into mRNP granules. As promoter sequences and translation occur in separate cellular compartments, this suggests that transcripts are co-transcriptionally imprinted in such a way to determine its cytoplasmic fate. While the exact factors that distinguish cytoplasmic fates remains unclear, it is hypothesized that these induced transcripts are either co-transcriptionally modified or bound to an unknown RBP that is sufficient to differentiate cytoplasmic fate. Furthermore, it is unclear whether these factors are individually responsible for translatability, localization, or both. Based on the model of RNA incorporation into mRNP granules and recent studies, it is suspected that translatability is the driving force for localization during stress conditions (Matheny et al. 2019). However, while a correlation is observed between translatability during stress and localization with respect to mRNP granules, it remains unclear whether translatability is either sufficient or necessary to drive localization or vice versa.

1.6 Dissertation Overview

While we have learned much about how cells mechanistically manipulate mRNA and translation to regulate their proteome, much study is needed to understand the nuances, controls, and factors involved in post-transcriptional regulation. In this dissertation, I explore factors involved in post-transcriptional regulation of protein synthesis using the budding yeast *Saccharomyces cerevisiae* as a model organism. In Chapter 2, I discuss the development of an assay designed to quantify the elongation rate of an *in vivo* reporter construct. We utilize this assay to assess the stalling duration of synonymous codon substitutions and strong, localized stalls. Our findings indicate that localized stalls negatively impact gene expression in a Hel2-dependent manner. Surprisingly, we find that while synonymous codon substitutions to nonoptimal codons also negatively impacts gene expression, this is through a non-Hel2-mediated mechanism. In Chapter 3, I examine the relationship between translatability and mRNA localization during acute glucose starvation. Section 3.2 investigates the proteins Rvb1 and Rvb2 as drivers of mRNP granule localization for a select subset of stress response genes. Section 3.3 briefly explores how mRNA localization of a reporter construct is altered by inhibition of translation. Taken together, these chapters contribute to a better mechanistic understanding of how protein synthesis is regulated in cells. Particularly, the development of our elongation assay will assist future researchers to develop a more quantified look at how elongation stalling is managed by cellular machinery.

1.7 References

1. Stouthamer, A. H. (1973). A theoretical study on the amount of ATP required for synthesis of microbial cell material. *Antonie van Leeuwenhoek*, *39*(1), 545-565.

2. Buttgereit, F., & Brand, M. D. (1995). A hierarchy of ATP-consuming processes in mammalian cells. *Biochemical Journal*, *312*(1), 163-167.

3. Wieser, W., & Krumschnabel, G. (2001). Hierarchies of ATP-consuming processes: direct compared with indirect measurements, and comparative aspects. *Biochemical Journal*, *355*(2), 389-395.

4. Hartley, H. (1951). Origin of the word 'protein'. *Nature*, *168*(4267), 244-244.

5. Audic, Y., & Hartley, R. S. (2004). Post-transcriptional regulation in cancer. *Biology of the Cell*, *96*(7), 479-498.

6. Corbett, A. H. (2018). Post-transcriptional regulation of gene expression and human disease. *Current opinion in cell biology*, *52*, 96-104.

7. Schaefke, B., Sun, W., Li, Y. S., Fang, L., & Chen, W. (2018). The evolution of posttranscriptional regulation. *Wiley Interdisciplinary Reviews: RNA*, *9*(5), e1485.

8. Obernosterer, G., Leuschner, P. J., Alenius, M., & Martinez, J. (2006). Post-transcriptional regulation of microRNA expression. *Rna*, *12*(7), 1161-1167.

9. Furlan, M., de Pretis, S., & Pelizzola, M. (2021). Dynamics of transcriptional and post-transcriptional regulation. *Briefings in Bioinformatics*, *22*(4), bbaa389.

10. Kim, W., & Kyung Lee, E. (2012). Post-transcriptional regulation in metabolic diseases. *RNA biology*, *9*(6), 772-780.

11. Lawless, C., Pearson, R. D., Selley, J. N., Smirnova, J. B., Grant, C. M., Ashe, M. P., Pavitt, G.D., & Hubbard, S. J. (2009). Upstream sequence elements direct post-transcriptional regulation of gene expression under stress conditions in yeast. *BMC genomics*, *10*(1), 1-20.

12. Beyer, A., Hollunder, J., Nasheuer, H. P., & Wilhelm, T. (2004). Post-transcriptional expression regulation in the yeast Saccharomyces cerevisiae on a genomic scale. *Molecular & cellular proteomics*, *3*(11), 1083-1092.

13. Kos-Braun, I. C., & Koš, M. (2017). Post-transcriptional regulation of ribosome biogenesis in yeast. *Microbial Cell*, *4*(5), 179.

14. McCarthy, J. E. (1998). Posttranscriptional control of gene expression in yeast. *Microbiology and Molecular Biology Reviews*, *62*(4), 1492-1553.

15. Pakos-Zebrucka, K., Koryga, I., Mnich, K., Ljujic, M., Samali, A., & Gorman, A. M. (2016). The integrated stress response. *EMBO reports*, *17*(10), 1374-1395.

16. Buxbaum, A. R., Haimovich, G., & Singer, R. H. (2015). In the right place at the right time: visualizing and understanding mRNA localization. *Nature reviews Molecular cell biology*, *16*(2), 95-109.

17. Grantham, R., Gautier, C., & Gouy, M. (1980). Codon frequencies in 119 individual genes confirm corsistent choices of degenerate bases according to genome type. *Nucleic acids research*, *8*(9), 1893-1912.

18. Bennetzen, J. L., & Hall, B. D. (1982). Codon selection in yeast. *Journal of Biological Chemistry*, *257*(6), 3026-3031.

19. Gouy, M., & Gautier, C. (1982). Codon usage in bacteria: correlation with gene expressivity. *Nucleic acids research*, *10*(22), 7055-7074.

20. Pechmann, S., & Frydman, J. (2013). Evolutionary conservation of codon optimality reveals hidden signatures of cotranslational folding. *Nature structural & molecular biology*, *20*(2), 237-243.

21. Reis, M. D., Savva, R., & Wernisch, L. (2004). Solving the riddle of codon usage preferences: a test for translational selection. *Nucleic acids research*, *32*(17), 5036-5044.

22. Presnyak, V., Alhusaini, N., Chen, Y. H., Martin, S., Morris, N., Kline, N., Olson, S., Weinberg, D., Baker, K. E., Graveley, B. R., & Coller, J. (2015). Codon optimality is a major determinant of mRNA stability. *Cell*, *160*(6), 1111-1124.

23. Radhakrishnan, A., Chen, Y. H., Martin, S., Alhusaini, N., Green, R., & Coller, J. (2016). The DEAD-box protein Dhh1p couples mRNA decay and translation by monitoring codon optimality. *Cell*, *167*(1), 122-132.

24. Harigaya, Y., & Parker, R. (2016). Codon optimality and mRNA decay. *Cell research*, *26*(12), 1269-1270.

25. Hanson, G., & Coller, J. (2018). Codon optimality, bias and usage in translation and mRNA decay. *Nature reviews Molecular cell biology*, *19*(1), 20-30.

26. Sørensen, M. A., & Pedersen, S. (1991). Absolute in vivo translation rates of individual codons in Escherichia coli: the two glutamic acid codons GAA and GAG are translated with a threefold difference in rate. *Journal of molecular biology*, *222*(2), 265-280.

27. Ingolia, N. T. (2014). Ribosome profiling: new views of translation, from single codons to genome scale. *Nature reviews genetics*, *15*(3), 205-213.

28. Ingolia, N. T., Ghaemmaghami, S., Newman, J. R., & Weissman, J. S. (2009). Genome-wide analysis in vivo of translation with nucleotide resolution using ribosome profiling. *science*, *324*(5924), 218-223.

29. Hussmann, J. A., Patchett, S., Johnson, A., Sawyer, S., & Press, W. H. (2015). Understanding biases in ribosome profiling experiments reveals signatures of translation dynamics in yeast. *PLoS genetics*, *11*(12), e1005732.

30. Gardin, J., Yeasmin, R., Yurovsky, A., Cai, Y., Skiena, S., & Futcher, B. (2014). Measurement of average decoding rates of the 61 sense codons in vivo. *Elife*, *3*, e03735.

31. Weinberg, D. E., Shah, P., Eichhorn, S. W., Hussmann, J. A., Plotkin, J. B., & Bartel, D. P. (2016). Improved ribosome-footprint and mRNA measurements provide insights into dynamics and regulation of yeast translation. *Cell reports*, *14*(7), 1787-1799.

32. Saikia, M., Wang, X., Mao, Y., Wan, J., Pan, T., & Qian, S. B. (2016). Codon optimality controls differential mRNA translation during amino acid starvation. *Rna*, *22*(11), 1719-1727.

33. Chu, D., Barnes, D. J., & Von Der Haar, T. (2011). The role of tRNA and ribosome competition in coupling the expression of different mRNAs in Saccharomyces cerevisiae. *Nucleic acids research*, *39*(15), 6705-6714.

34. Koutmou, K. S., Radhakrishnan, A., & Green, R. (2015). Synthesis at the speed of codons. *Trends in biochemical sciences*, *40*(12), 717-718.

35. Letzring, D. P., Dean, K. M., & Grayhack, E. J. (2010). Control of translation efficiency in yeast by codon–anticodon interactions. *Rna*, *16*(12), 2516-2528.

36. Kisly, I., Kattel, C., Remme, J., & Tamm, T. (2021). Luciferase-based reporter system for in vitro evaluation of elongation rate and processivity of ribosomes. *Nucleic acids research*, *49*(10), e59-e59.

37. Thanaraj, T. A., & Argos, P. (1996). Protein secondary structural types are differentially coded on messenger RNA. *Protein science*, *5*(10), 1973-1983.

38. Yu, C. H., Dang, Y., Zhou, Z., Wu, C., Zhao, F., Sachs, M. S., & Liu, Y. (2015). Codon usage influences the local rate of translation elongation to regulate co-translational protein folding. *Molecular cell*, *59*(5), 744-754.

39. Xu, Y., Liu, K., Han, Y., Xing, Y., Zhang, Y., Yang, Q., & Zhou, M. (2021). Codon usage bias regulates gene expression and protein conformation in yeast expression system P. pastoris. *Microbial cell factories*, *20*(1), 1-15.

40. Collart, M. A., & Weiss, B. (2020). Ribosome pausing, a dangerous necessity for co-translational events. *Nucleic acids research*, *48*(3), 1043-1055.

41. Komar, A. A., Lesnik, T., & Reiss, C. (1999). Synonymous codon substitutions affect ribosome traffic and protein folding during in vitro translation. *FEBS letters*, *462*(3), 387-391.

42. Zhang, G., Hubalewska, M., & Ignatova, Z. (2009). Transient ribosomal attenuation coordinates protein synthesis and co-translational folding. *Nature structural & molecular biology*, *16*(3), 274-280.

43. Gamble, C. E., Brule, C. E., Dean, K. M., Fields, S., & Grayhack, E. J. (2016). Adjacent codons act in concert to modulate translation efficiency in yeast. *Cell*, *166*(3), 679-690.

44. Yang, J. R., Chen, X., & Zhang, J. (2014). Codon-by-codon modulation of translational speed and accuracy via mRNA folding. *PLoS biology*, *12*(7), e1001910.

45. Karpinets, T. V., Greenwood, D. J., Sams, C. E., & Ammons, J. T. (2006). RNA: protein ratio of the unicellular organism as a characteristic of phosphorous and nitrogen stoichiometry and of the cellular requirement of ribosomes for protein synthesis. *BMC biology*, *4*(1), 1-10.

46. Riba, A., Di Nanni, N., Mittal, N., Arhné, E., Schmidt, A., & Zavolan, M. (2019). Protein synthesis rates and ribosome occupancies reveal determinants of translation elongation rates. *Proceedings of the national academy of sciences*, *116*(30), 15023-15032.

47. Han, P., Shichino, Y., Schneider-Poetsch, T., Mito, M., Hashimoto, S., Udagawa, T., Kohno, K., Yoshida, M., Mishima, Y., Inada, T., & Iwasaki, S. (2020). Genome-wide survey of ribosome collision. *Cell reports*, *31*(5), 107610.

48. Arpat, A. B., Liechti, A., De Matos, M., Dreos, R., Janich, P., & Gatfield, D. (2020). Transcriptome-wide sites of collided ribosomes reveal principles of translational pausing. *Genome research*, *30*(7), 985-999.

49. Zhao, T., Chen, Y. M., Li, Y., Wang, J., Chen, S., Gao, N., & Qian, W. (2021). Disome-seq reveals widespread ribosome collisions that promote cotranslational protein folding. *Genome biology*, *22*(1), 1-35.

50. Goldman, D. H., Livingston, N. M., Movsik, J., Wu, B., & Green, R. (2021). Live-cell imaging reveals kinetic determinants of quality control triggered by ribosome stalling. *Molecular cell*, *81*(8), 1830-1840.

51. Kapur, M., & Ackerman, S. L. (2018). mRNA translation gone awry: translation fidelity and neurological disease. *Trends in Genetics*, *34*(3), 218-231.

52. Chu, J., Hong, N. A., Masuda, C. A., Jenkins, B. V., Nelms, K. A., Goodnow, C. C., Glynne, R. J., Wu, H., Masliah, E., Joazeiro, C. A., & Kay, S. A. (2009). A mouse forward genetics screen identifies LISTERIN as an E3 ubiquitin ligase

involved in neurodegeneration. *Proceedings of the National Academy of Sciences*, *106*(7), 2097-2103.

53. Choe, Y. J., Park, S. H., Hassemer, T., Körner, R., Vincenz-Donnelly, L., Hayer-Hartl, M., & Hartl, F. U. (2016). Failure of RQC machinery causes protein aggregation and proteotoxic stress. *Nature*, *531*(7593), 191-195.

54. Nedialkova, D. D., & Leidel, S. A. (2015). Optimization of codon translation rates via tRNA modifications maintains proteome integrity. *Cell*, *161*(7), 1606-1618.

55. Yonashiro, R., Tahara, E. B., Bengtson, M. H., Khokhrina, M., Lorenz, H., Chen, K. C., Kigoshi-Tansho, Y., Savas, J. N., Yates III, J. R., Kay, S. A., Craig, E. A., Mogk, A., Bukau, B., & Joazeiro, C. A. (2016). The Rqc2/Tae2 subunit of the ribosome-associated quality control (RQC) complex marks ribosome-stalled nascent polypeptide chains for aggregation. *Elife*, *5*, e11794.

56. Doma, M. K., & Parker, R. (2006). Endonucleolytic cleavage of eukaryotic mRNAs with stalls in translation elongation. *Nature*, *440*(7083), 561-564.

57. Letzring, D. P., Wolf, A. S., Brule, C. E., & Grayhack, E. J. (2013). Translation of CGA codon repeats in yeast involves quality control components and ribosomal protein L1. *Rna*, *19*(9), 1208-1217.

58. Simms, C. L., Hudson, B. H., Mosior, J. W., Rangwala, A. S., & Zaher, H. S. (2014). An active role for the ribosome in determining the fate of oxidized mRNA. *Cell reports*, *9*(4), 1256-1264.

59. Yip, M. C., & Shao, S. (2021). Detecting and Rescuing Stalled Ribosomes. *Trends in Biochemical Sciences*.

60. Meydan, S., & Guydosh, N. R. (2020). Disome and trisome profiling reveal genome-wide targets of ribosome quality control. *Molecular cell*, *79*(4), 588-602.

61. Chandrasekaran, V., Juszkiewicz, S., Choi, J., Puglisi, J. D., Brown, A., Shao, S., Ramakrishnan, V., & Hegde, R. S. (2019). Mechanism of ribosome stalling during translation of a poly (A) tail. *Nature structural & molecular biology*, *26*(12), 1132-1140.

62. Hellen, C. U. (2018). Translation termination and ribosome recycling in eukaryotes. *Cold Spring Harbor perspectives in biology*, *10*(10), a032656.

63. Dever, T. E., & Green, R. (2012). The elongation, termination, and recycling phases of translation in eukaryotes. *Cold Spring Harbor perspectives in biology*, *4*(7), a013706.

64. Mitkevich, V. A., Kononenko, A. V., Petrushanko, I. Y., Yanvarev, D. V., Makarov, A. A., & Kisselev, L. L. (2006). Termination of translation in eukaryotes is mediated by the quaternary eRF1• eRF3• GTP• Mg2+ complex. The biological

roles of eRF3 and prokaryotic RF3 are profoundly distinct. *Nucleic acids research*, *34*(14), 3947-3954.

65. Jackson, R. J., Hellen, C. U., & Pestova, T. V. (2012). Termination and post-termination events in eukaryotic translation. *Advances in protein chemistry and structural biology*, *86*, 45-93.

66. Van Hoof, A., & Wagner, E. J. (2011). A brief survey of mRNA surveillance. *Trends in biochemical sciences*, *36*(11), 585-592.

67. Shoemaker, C. J., & Green, R. (2012). Translation drives mRNA quality control. *Nature structural & molecular biology*, *19*(6), 594-601.

68. Ikeuchi, K., Tesina, P., Matsuo, Y., Sugiyama, T., Cheng, J., Saeki, Y., Tanaka, K., Becker, T., Beckmann, R. & Inada, T. (2019). Collided ribosomes form a unique structural interface to induce Hel2-driven quality control pathways. *The EMBO journal*, *38*(5), e100276.

69. Pechmann, S., Willmund, F., & Frydman, J. (2013). The ribosome as a hub for protein quality control. *Molecular cell*, *49*(3), 411-421.

70. Joazeiro, C. A. (2019). Mechanisms and functions of ribosome-associated protein quality control. *Nature Reviews Molecular Cell Biology*, *20*(6), 368-383.

71. Brandman, O., & Hegde, R. S. (2016). Ribosome-associated protein quality control. *Nature structural & molecular biology*, *23*(1), 7-15.

72. Meydan, S., & Guydosh, N. R. (2020). A cellular handbook for collided ribosomes: surveillance pathways and collision types. *Current genetics*, 1-8.

73. Matsuo, Y., Ikeuchi, K., Saeki, Y., Iwasaki, S., Schmidt, C., Udagawa, T., Sato, F., Tsuchiya, H., Becker, T., Tanaka, K., Ingolia, N. T., Beckmann, R., & Inada, T. (2017). Ubiquitination of stalled ribosome triggers ribosome-associated quality control. *Nature communications*, *8*(1), 1-14.

74. Sitron, C. S., Park, J. H., & Brandman, O. (2017). Asc1, Hel2, and Slh1 couple translation arrest to nascent chain degradation. *Rna*, *23*(5), 798-810.

75. Hashimoto, S., Sugiyama, T., Yamazaki, R., Nobuta, R., & Inada, T. (2020). Identification of a novel trigger complex that facilitates ribosome-associated quality control in mammalian cells. *Scientific reports*, *10*(1), 1-12.

76. Juszkiewicz, S., Speldewinde, S. H., Wan, L., Svejstrup, J. Q., & Hegde, R. S. (2020). The ASC-1 complex disassembles collided ribosomes. *Molecular cell*, *79*(4), 603-614.

77. Inada, T. (2020). Quality controls induced by aberrant translation. *Nucleic acids research*, *48*(3), 1084-1096.

78. Brandman, O., Stewart-Ornstein, J., Wong, D., Larson, A., Williams, C. C., Li, G. W., Zhou, S., King, D., Shen, P. S., Weibezahn, J., Dunn, J. D., Rouskin, S., Inada, T., Frost, A., & Weissman, J. S. (2012). A ribosome-bound quality control complex triggers degradation of nascent peptides and signals translation stress. *Cell*, *151*(5), 1042-1054.

79. Shen, P. S., Park, J., Qin, Y., Li, X., Parsawar, K., Larson, M. H., Cox, J., Cheng, Y., Lambowitz, A. M., Weissman, J. S., Brandman, O., & Frost, A. (2015). Rqc2p and 60S ribosomal subunits mediate mRNA-independent elongation of nascent chains. *Science*, *347*(6217), 75-78.

80. Shao, S., Brown, A., Santhanam, B., & Hegde, R. S. (2015). Structure and assembly pathway of the ribosome quality control complex. *Molecular Cell*, *57*(3), 433-444.

81. Bengtson, M. H., & Joazeiro, C. A. (2010). Role of a ribosome-associated E3 ubiquitin ligase in protein quality control. *nature*, *467*(7314), 470-473.

82. Matsuda, R., Ikeuchi, K., Nomura, S., & Inada, T. (2014). Protein quality control systems associated with no-go and n onstop m RNA surveillance in yeast. *Genes to Cells*, *19*(1), 1-12.

83. Joazeiro, C. A. (2017). Ribosomal stalling during translation: providing substrates for ribosome-associated protein quality control. *Annual review of cell and developmental biology*, *33*, 343-368.

84. Pisareva, V. P., Skabkin, M. A., Hellen, C. U., Pestova, T. V., & Pisarev, A. V. (2011). Dissociation by Pelota, Hbs1 and ABCE1 of mammalian vacant 80S ribosomes and stalled elongation complexes. *The EMBO journal*, *30*(9), 1804-1817.

85. Shoemaker, C. J., Eyler, D. E., & Green, R. (2010). Dom34: Hbs1 promotes subunit dissociation and peptidyl-tRNA drop-off to initiate no-go decay. *Science*, *330*(6002), 369-372.

86. Shoemaker, C. J., & Green, R. (2011). Kinetic analysis reveals the ordered coupling of translation termination and ribosome recycling in yeast. *Proceedings of the National Academy of Sciences*, *108*(51), E1392-E1398.

87. Harigaya, Y., & Parker, R. (2010). No-go decay: a quality control mechanism for RNA in translation. *Wiley Interdisciplinary Reviews: RNA*, *1*(1), 132-141.

88. Simms, C. L., Yan, L. L., & Zaher, H. S. (2017). Ribosome collision is critical for quality control during no-go decay. *Molecular cell*, *68*(2), 361-373.

89. Simms, C. L., Thomas, E. N., & Zaher, H. S. (2017). Ribosome-based quality control of mRNA and nascent peptides. *Wiley Interdisciplinary Reviews: RNA*, *8*(1), e1366.

90. D'Orazio, K. N., Wu, C. C. C., Sinha, N., Loll-Krippleber, R., Brown, G. W., & Green, R. (2019). The endonuclease Cue2 cleaves mRNAs at stalled ribosomes during No Go Decay. *Elife*, *8*, e49117.

91. Powers, K. T., Szeto, J. Y. A., & Schaffitzel, C. (2020). New insights into no-go, non-stop and nonsense-mediated mRNA decay complexes. *Current Opinion in Structural Biology*, *65*, 110-118.

92. Buskirk, A. R., & Green, R. (2017). Ribosome pausing, arrest and rescue in bacteria and eukaryotes. *Philosophical Transactions of the Royal Society B: Biological Sciences*, *372*(1716), 20160183.

93. Navickas, A., Chamois, S., Saint-Fort, R., Henri, J., Torchet, C., & Benard, L. (2020). No-Go Decay mRNA cleavage in the ribosome exit tunnel produces 5′-OH ends phosphorylated by Trl1. *Nature communications*, *11*(1), 1-11.

94. Garzia, A., Jafarnejad, S. M., Meyer, C., Chapat, C., Gogakos, T., Morozov, P., Amiri, M., Shapiro, M., Molina, H., Tuschl, T., & Sonenberg, N. (2017). The E3 ubiquitin ligase and RNA-binding protein ZNF598 orchestrates ribosome quality control of premature polyadenylated mRNAs. *Nature communications*, *8*(1), 1-10.

95. Juszkiewicz, S., & Hegde, R. S. (2017). Initiation of quality control during poly (A) translation requires site-specific ribosome ubiquitination. *Molecular cell*, *65*(4), 743-750.

96. Kloc, M., Zearfoss, N. R., & Etkin, L. D. (2002). Mechanisms of subcellular mRNA localization. *Cell*, *108*(4), 533-544.

97. Jansen, R. P. (2001). mRNA localization: message on the move. *Nature reviews Molecular cell biology*, *2*(4), 247-256.

98. Martin, K. C., & Ephrussi, A. (2009). mRNA localization: gene expression in the spatial dimension. *Cell*, *136*(4), 719-730.

99. Jambhekar, A., & DeRisi, J. L. (2007). Cis-acting determinants of asymmetric, cytoplasmic RNA transport. *Rna*, *13*(5), 625-642.

100. Shahbabian, K., & Chartrand, P. (2012). Control of cytoplasmic mRNA localization. *Cellular and Molecular Life Sciences*, *69*(4), 535-552.

101. Patel, V. L., Mitra, S., Harris, R., Buxbaum, A. R., Lionnet, T., Brenowitz, M., Girvin, M., Levy, M., Almo, S. C., Singer, R. H., & Chao, J. A. (2012). Spatial arrangement of an RNA zipcode identifies mRNAs under post-transcriptional control. *Genes & development*, *26*(1), 43-53.

102. Forrest, K. M., & Gavis, E. R. (2003). Live imaging of endogenous RNA reveals a diffusion and entrapment mechanism for nanos mRNA localization in Drosophila. *Current biology*, *13*(14), 1159-1168.

103. Gavis, E. R., & Lehmann, R. (1992). Localization of nanos RNA controls embryonic polarity. *Cell*, *71*(2), 301-313.

104. Long, R. M., Singer, R. H., Meng, X., Gonzalez, I., Nasmyth, K., & Jansen, R. P. (1997). Mating type switching in yeast controlled by asymmetric localization of ASH1 mRNA. *Science*, *277*(5324), 383-387.

105. Garner, C. C., Tucker, R. P., & Matus, A. (1988). Selective localization of messenger RNA for cytoskeletal protein MAP2 in dendrites. *Nature*, *336*(6200), 674-677.

106. Lécuyer, E., Yoshida, H., Parthasarathy, N., Alm, C., Babak, T., Cerovina, T., Hughes, T. R., Tomancak, P., & Krause, H. M. (2007). Global analysis of mRNA localization reveals a prominent role in organizing cellular architecture and function. *Cell*, *131*(1), 174-187.

107. Cajigas, I. J., Tushev, G., Will, T. J., tom Dieck, S., Fuerst, N., & Schuman, E. M. (2012). The local transcriptome in the synaptic neuropil revealed by deep sequencing and high-resolution imaging. *Neuron*, *74*(3), 453-466.

108. Eliscovich, C., Buxbaum, A. R., Katz, Z. B., & Singer, R. H. (2013). mRNA on the move: the road to its biological destiny. *Journal of Biological Chemistry*, *288*(28), 20361-20368.

109. Zaessinger, S., Busseau, I., & Simonelig, M. (2006). Oskar allows nanos mRNA translation in Drosophila embryos by preventing its deadenylation by Smaug/CCR4.

110. Jain, R. A., & Gavis, E. R. (2008). The Drosophila hnRNP M homolog Rumpelstiltskin regulates nanos mRNA localization.

111. Becalska, A. N., Kim, Y. R., Belletier, N. G., Lerit, D. A., Sinsimer, K. S., & Gavis, E. R. (2011). Aubergine is a component of a nanos mRNA localization complex. *Developmental biology*, *349*(1), 46-52.

112. Böhl, F., Kruse, C., Frank, A., Ferring, D., & Jansen, R. P. (2000). She2p, a novel RNA-binding protein tethers ASH1 mRNA to the Myo4p myosin motor via She3p. *The EMBO journal*, *19*(20), 5514-5524.

113. Deng, Y., Singer, R. H., & Gu, W. (2008). Translation of ASH1 mRNA is repressed by Puf6p–Fun12p/eIF5B interaction and released by CK2 phosphorylation. *Genes & development*, *22*(8), 1037-1050.

114. Bobola, N., Jansen, R. P., Shin, T. H., & Nasmyth, K. (1996). Asymmetric accumulation of Ash1p in postanaphase nuclei depends on a myosin and restricts yeast mating-type switching to mother cells. *Cell*, *84*(5), 699-709.

115. Gonzalez, I., Buonomo, S. B., Nasmyth, K., & von Ahsen, U. (1999). ASH1 mRNA localization in yeast involves multiple secondary structural elementsand Ash1 protein translation. *Current biology*, *9*(6), 337-340.

116. Besse, F., & Ephrussi, A. (2008). Translational control of localized mRNAs: restricting protein synthesis in space and time. *Nature reviews Molecular cell biology*, *9*(12), 971-980.

117. Abaza, I., & Gebauer, F. (2008). Trading translation with RNA-binding proteins. *Rna*, *14*(3), 404-409.

118. Ogg, S. C., & Walter, P. (1995). SRP samples nascent chains for the presenceof signal sequences by interacting with ribosomes at a discrete step during translation elongation. *Cell*, *81*(7), 1075-1084.

119. Kapp, K., Schrempf, S., Lemberg, M. K., & Dobberstein, B. (2009). Post-targeting functions of signal peptides. *Protein transport into the endoplasmic reticulum*, 1-16.

120. Walter, P., Ibrahimi, I., & Blobel, G. U. N. T. E. R. (1981). Translocation of proteins across the endoplasmic reticulum. I. Signal recognition protein (SRP) binds to in-vitro-assembled polysomes synthesizing secretory protein. *Journal of Cell Biology*, *91*(2), 545-550.

121. Tisdale, S., & Pellizzoni, L. (2017). RNA-processing dysfunction in spinal muscular atrophy. In *Spinal Muscular Atrophy* (pp. 113-131). Academic Press.

122. Walter, P., & Blobel, G. (1983). Subcellular distribution of signal recognition particle and 7SL-RNA determined with polypeptide-specific antibodies and complementary DNA probe. *The Journal of cell biology*, *97*(6), 1693-1699.

123. Gilmore, R., Blobel, G., & Walter, P. (1982). Protein translocation across the endoplasmic reticulum. I. Detection in the microsomal membrane of a receptor for the signal recognition particle. *The Journal of cell biology*, *95*(2), 463-469.

124. Lütcke, H. (1995). Signal recognition particle (SRP), a ubiquitous initiator of protein translocation. *European journal of biochemistry*, *228*(3), 531-550.

125. Luirink, J., & Sinning, I. (2004). SRP-mediated protein targeting: structure and function revisited. *Biochimica et Biophysica Acta (BBA)-Molecular Cell Research*, *1694*(1-3), 17-35.

126. Siegel, V., & Walter, P. (1985). Elongation arrest is not a prerequisite for secretory protein translocation across the microsomal membrane. *The Journal of cell biology*, *100*(6), 1913-1921.

127. Siegel, V., & Walter, P. (1988). Each of the activities of signal recognition particle (SRP) is contained within a distinct domain: analysis of biochemical mutants of SRP. *Cell*, *52*(1), 39-49.

128. Mason, N., Ciufo, L. F., & Brown, J. D. (2000). Elongation arrest is a physiologically important function of signal recognition particle. *The EMBO journal*, *19*(15), 4164-4174.

129. Tsuboi, T., Viana, M. P., Xu, F., Yu, J., Chanchani, R., Arceo, X. G., Tutucci, E., Choi, J., Chen, Y. S., Singer, R. H., Rafelski, S. M., & Zid, B. M. (2020). Mitochondrial volume fraction and translation duration impact mitochondrial mRNA localization and protein synthesis. *Elife*, *9*, e57814.

130. Tsuboi, T., Leff, J., & Zid, B. M. (2020). Post-transcriptional control of mitochondrial protein composition in changing environmental conditions. *Biochemical Society Transactions*, *48*(6), 2565-2578.

131. Buchan, J. R., & Parker, R. (2009). Eukaryotic stress granules: the ins and outs of translation. *Molecular cell*, *36*(6), 932-941.

132. Khong, A., Matheny, T., Jain, S., Mitchell, S. F., Wheeler, J. R., & Parker, R. (2017). The stress granule transcriptome reveals principles of mRNA accumulation in stress granules. *Molecular cell*, *68*(4), 808-820.

133. Teixeira, D., Sheth, U., Valencia-Sanchez, M. A., Brengues, M., & Parker, R. (2005). Processing bodies require RNA for assembly and contain nontranslating mRNAs. *Rna*, *11*(4), 371-382.

134. Jain, S., Wheeler, J. R., Walters, R. W., Agrawal, A., Barsic, A., & Parker, R. (2016). ATPase-modulated stress granules contain a diverse proteome and substructure. *Cell*, *164*(3), 487-498.

135. Guzikowski, A. R., Chen, Y. S., & Zid, B. M. (2019). Stress-induced mRNP granules: form and function of processing bodies and stress granules. *Wiley Interdisciplinary Reviews: RNA*, *10*(3), e1524.

136. Protter, D. S., & Parker, R. (2016). Principles and properties of stress granules. *Trends in cell biology*, *26*(9), 668-679.

137. Corbet, G. A., & Parker, R. (2019, January). RNP Granule Formation: Lessons from P-Bodies and stress granules. In *Cold Spring Harbor Symposia on Quantitative Biology* (Vol. 84, pp. 203-215). Cold Spring Harbor Laboratory Press.

138. Van Treeck, B., & Parker, R. (2019). Principles of stress granules revealed by imaging approaches. *Cold Spring Harbor perspectives in biology*, *11*(2), a033068.

139. Chernov, K. G., Barbet, A., Hamon, L., Ovchinnikov, L. P., Curmi, P. A., & Pastré, D. (2009). Role of microtubules in stress granule assembly. *Journal of Biological Chemistry*, *284*(52), 36569-36580.

140. Begovich, K., & Wilhelm, J. E. (2020). An in vitro assembly system identifies roles for RNA nucleation and ATP in yeast stress granule formation. *Molecular Cell*, *79*(6), 991-1007.

141. Buchan, J. R., Nissan, T., & Parker, R. (2010). Analyzing P-bodies and stress granules in Saccharomyces cerevisiae. *Methods in enzymology*, *470*, 619-640.

142. Lin, Y., Protter, D. S., Rosen, M. K., & Parker, R. (2015). Formation and maturation of phase-separated liquid droplets by RNA-binding proteins. *Molecular cell*, *60*(2), 208-219.

143. Van Treeck, B., Protter, D. S., Matheny, T., Khong, A., Link, C. D., & Parker, R. (2018). RNA self-assembly contributes to stress granule formation and defining the stress granule transcriptome. *Proceedings of the National Academy of Sciences*, *115*(11), 2734-2739.

144. Protter, D. S., Rao, B. S., Van Treeck, B., Lin, Y., Mizoue, L., Rosen, M. K., & Parker, R. (2018). Intrinsically disordered regions can contribute promiscuous interactions to RNP granule assembly. *Cell reports*, *22*(6), 1401-1412.

145. Van Treeck, B., & Parker, R. (2018). Emerging roles for intermolecular RNA-RNA interactions in RNP assemblies. *Cell*, *174*(4), 791-802.

146. Matheny, T., Rao, B. S., & Parker, R. (2019). Transcriptome-wide comparison of stress granules and P-bodies reveals that translation plays a major role in RNA partitioning. *Molecular and Cellular Biology*, *39*(24), e00313-19.

147. Wheeler, J. R., Matheny, T., Jain, S., Abrisch, R., & Parker, R. (2016). Distinct stages in stress granule assembly and disassembly. *Elife*, *5*, e18413.

148. Molliex, A., Temirov, J., Lee, J., Coughlin, M., Kanagaraj, A. P., Kim, H. J., Mittag, T., & Taylor, J. P. (2015). Phase separation by low complexity domains promotes stress granule assembly and drives pathological fibrillization. *Cell*, *163*(1), 123-133.

149. Zid, B. M., & O'Shea, E. K. (2014). Promoter sequences direct cytoplasmic localization and translation of mRNAs during starvation in yeast. *Nature*, *514*(7520), 117-121.

CHAPTER 2: Quantification of elongation stalls and impact on gene expression

2.1 Abstract

Ribosomal pauses are a critical part of co-translational events including protein folding and localization. However, extended ribosome pauses can lead to ribosome collisions, resulting in the activation of ribosome rescue pathways and turnover of protein and mRNA. While this relationship has been known, the specific threshold between permissible pausing versus activation of rescue pathways has not been quantified. We have taken a method used to measure elongation time and adapted it for use in *S. cerevisiae* to quantify the impact of elongation stalls. We find that in transcripts containing a strong, localized stall, a Hel2-mediated dose-dependent decrease in protein and mRNA expression and increase in elongation delay. In transcripts containing synonymous substitutions to nonoptimal codons, we find a decrease in protein and mRNA expression and similar increase in elongation delay but through a non-Hel2-mediated mechanism. This indicates that different distributions of poor codons in a transcript will activate different rescue pathways despite similar elongation stall durations. Finally, we find that Dhh1 selectively increases protein expression, mRNA expression, and elongation rate. Taken together, these results provide new quantitative mechanistic insight into the surveillance of translation and the roles of Hel2 and Dhh1 in mediating ribosome pausing events.

2.2 Introduction

Production of cellular proteins through translation is crucial for maintaining homeostasis and adapting to changing environmental conditions. Translation can be broken down into three sequential steps: initiation, during which ribosomes assemble at the initiation site on an mRNA, elongation, during which ribosomes translocate across the mRNA and build upon a nascent peptide, and termination, during which ribosomes are removed from the mRNA, recycled, and the newly synthesized protein is released. Cells dedicate many resources to the monitoring, regulation, and quality control of protein synthesis as dysregulation may lead to aberrant cellular function and neurological diseases such as ALS (Bosco 2018, Wang et al. 2016).

Each step in the translation process is governed by various regulatory steps. Initiation has long been known to be the rate-limiting step in translation and subject to intense regulation (Sonenberg and Hinnebusch 2009, Shah et al. 2013). Recent studies have focused on elongation as another important regulatory step in protein synthesis. Indeed, modulation of elongation speed has been shown to serve a functional role in both proper protein folding (Pechmann and Frydman 2013, Spencer et al. 2012, Yu et al. 2015, Zhao et al. 2021, Hartl et al. 2011) and localization (Tsuboi et al. 2020, Alamo et al. 2011, Ogg and Walter 1995, Mason et al. 2000). These examples give credence to the notion that ribosome pausing is essential for certain cellular processes. Recent reports using ribosome profiling to analyze disome peaks have estimated that upwards of 10% of translating ribosomes are engaged in the disome state (Zhao et al. 2021, Arpat et al. 2020, Han et al. 2020), indicating the commonplace occurrence of ribosome collisions.

The functional and necessary nature of ribosome stalls, however, makes it challenging for cellular machinery to distinguish between beneficial stalls and situations requiring ribosome rescue. Ribosomes that undergo translation on an aberrant mRNA, such as on a truncated mRNA, stall in place and are unable to be disassembled by translation termination machinery (Buskirk and Green 2017, Yip and Shao 2021, Joazeiro 2017). Upon extended stalling events, translating ribosomes may collide with stalled ribosomes, resulting in a ribosome collision which can eventually lead to further accumulation of collided ribosomes. Two pathways may be activated upon the detection of these collision events: (1) ribosome quality control (RQC), which leads to the rescue and recycling of stalled ribosomes, and (2) no-go decay (NGD), which leads to the endonucleolytic cleavage and subsequent degradation of the aberrant transcript. Both pathways are triggered by the ribosome collision sensor Hel2(yeast)/ZNF598(mammals) which detects disome formations which form as a result of prolonged ribosome stalling (Ikeuchi et al. 2019). In RQC, Hel2 ubiquitinates the small ribosomal subunit which leads to activation of the RQC trigger (RQT) complex in yeast, ultimately resulting in ribosome disassembly and degradation of the nascent peptide (Buskirk and Green 2017, Yip and Shao 2021, Joazeiro 2017). Concurrently, Hel2 activation also leads to the activation of the NGD pathway which results in mRNA degradation primarily through the endonuclease Cue2 and the exonucleases Xrn1 and Ski7 (Buskirk and Green 2017, D'Orazio et al. 2019, Navickas et al. 2020). Hel2 and other sensors of elongation quality must maintain a balance between permitting transient and functional stalls while at the same time engaging rescue pathways to prevent the buildup of ribosomes on problematic mRNA.

How elongation quality sensors are able to distinguish between functional stalls and those requiring rescue pathways remains unclear. It has been proposed that the severity of ribosome collision may determine which cellular response is activated in response to a collision event (Meydan and Guydosh 2020). While this model may explain how functional stalls and detrimental stalls either resume elongation or initiate RQC using the same surveillance pathways, respectively, the definition of “severity” in this context remains vague. Are the distinguishing factors the time duration of the stall, the number of ribosome collisions, the specific location and context of where the stall occurs on a transcript, or a combination of all these factors and more? It is from this lack of understanding of how cellular surveillance machinery is able to distinguish between these two opposing outcomes that necessitates reliable, quantitative methods to describe the various aspects of ribosome stalling events.

One important factor that contributes to elongation speed is codon optimality, a metric that describes the translational efficiency of the 61 amino acid specifying codons. Codon optimality, unique to each species, takes into account various factors implicated in elongation rate, including tRNA availability and demand, frequency of use in the genome, GC content, and interactions with the ribosome exit tunnel (Presnyak et al. 2015, Reis et al. 2004, Gardin et al. 2014, Pechmann et al. 2013). Furthermore, codon optimality has been found to correlate with elongation speed and mRNA decay, with transcripts enriched in “optimal” codons associated with faster elongation speed and lower mRNA decay rates and those enriched in “nonoptimal” codons associated with slower elongation speed and higher mRNA decay rates (Radhakrishnan et al. 2016, Harigaya and Parker 2016, Hanson and Coller 2018, Ingolia 2014, Ingolia et al. 2009,

Hussman et al. 2015, Gardin et al. 2014, Weinberg et al. 2016, Saikia et al. 2016, Chu et al. 2011, Koutmou et al. 2015). While many studies, both *in vivo* and *in vitro*, have assessed the impact of synonymous codon substitutions on protein expression, mRNA decay, and ribosome pausing, quantification of the impact on elongation time has not been widely available.

In this study, we describe the development of an *in vivo* quantitative luciferase-based assay to measure elongation time. We assessed the time delay associated with acute stalls caused by the inclusion of repeats of the nonoptimal arginine codon CGA and find that elongation time increases in a dose-dependent manner. Surprisingly, we find that no go RNA decay reaches a maximum level at a specific stall length despite increasing translation elongation times and protein expression continuing to decrease. Furthermore, we assessed the effect of synonymous codon substitutions on elongation time of a standardized ORF and identified the leucine codon CTT as a strong driver of elongation delay. CTT's effect on elongation time is dependent on its inclusion in the 5' end of the ORF. The development of this assay and our findings provide steps towards a detailed understanding of the triggers of ribosome quality control pathways.

2.3 Results

2.3.1 Development and validation of elongation assay

To create a quantitative elongation duration reporter assay, we utilized a tetracycline-inducible promoter to control mRNA induction of a bioluminescent nanoluciferase (nLuc) reporter downstream of open reading frames (ORFs) of interest. The nLuc reporter has been previously studied in yeast under the control of a stress-

inducible promoter and its bioluminescent output faithfully recapitulates induced mRNA levels after heat shock (Masser et al. 2016). To test this system, we developed a series of constructs in which we varied the length of the upstream ORF by insertion of yeast-optimized yellow fluorescent protein (YFP) or yeast-optimized monomeric infrared red fluorescent protein (miRFP) ORFs upstream of nLuc (Figure 2.3.1A). nLuc protein expression was collected for each construct over 60 minutes and normalized to OD600 measured at T=0 min. Elongation time was calculated using a Schleif plot (Schleif et al. 1973) and adjusted based on an average mRNA transcription time of 1500 nucleotides per second (Mason and Struhl 2005, Edwards et al. 1991). We find a delay in the first appearance of nLuc upon the addition of optYFP and a further delay in the longer miRFP-optYFP-nLuc reporter (Figure 2.3.1B). We then used these measured delays to calculate the translation elongation rate of optYFP and miRFP ORFs as approximately 4 AA/sec and 3 AA/sec (Figure 2.3.1C), respectively, which is consistent with bulk elongation rate measurements of 3-10 AA/sec (Karpinets et al. 2006, Riba et al. 2019). We do not find a significant difference in elongation rate between the two optimized ORFs. This implies that our reporter can quantify the in vivo translation rates of our reporters.

2.3.2 Hel2 decreases protein expression, mRNA expression, and delays elongation in acute CGA constructs

To quantify the duration of elongation pauses and assess their impact on gene expression, we classified elongation stalls into two categories: (1) acute stalls, which are characterized by a strong, localized internal stall made of nonoptimal codons within

the ORF and (2) distributed stalls, which are characterized by nonoptimal codons distributed throughout the ORF (Figure 2.3.2). To measure the effect of acute stalls on elongation time and gene expression, we developed a series of constructs in which we inserted between 2 and 6 tandem CGA repeats between the yeast-optimized YFP ORF and nLuc reporter ORF shown previously (Figure 2.3.3A). CGA codons have been previously shown to induce ribosomal stalling and reduce protein expression (Letzring et al. 2010, Veltri et al. 2021). First, we tested the protein expression of our induced constructs and found a dose-dependent exponential decline in protein production as the number of CGA codons increased, similar to a previous study by Letzring and colleagues (Letzring 2010) (Figure 2.3.3B). We however, did not see an impact on protein expression until 3 CGA codons were included. Next, we measured mRNA expression and found that mRNA expression significantly decreased with the addition of 3 CGA codons but mRNA levels remained constant around 40% of our control construct regardless of additional CGA codons (Figure 2.3.3C). We then measured the elongation delay in each of our constructs by comparing to a control reporter lacking any CGA codons (Figure 2.3.3D). We found that elongation delay increased in a dose-dependent manner beginning at 3xCGAs, with 6xCGA causing an ~4.5 minute extension of the translation duration. There was a relatively linear relationship between CGA stall number after 3 CGAs and elongation time which allowed us to calculate that each CGA adds approximately 76 seconds to the overall elongation time.

We then asked whether the impact on gene expression seen in our CGA-containing strains was a result of Hel2-mediated effects. Hel2 is a translation surveillance factor that senses ribosome collisions and activates the ribosome rescue

pathways ribosome quality control (RQC) and no-go decay (NGD) pathways which result in protein and mRNA turnover, respectively. We measured protein expression in our constructs containing 2, 4, and 6 CGAs in a ΔHel2 background and we compared it to their wild type (WT) counterparts (Figure 2.3.4A). We found that deletion of Hel2 partially rescued protein expression in the 4xCGA and 6xCGA. We next measured RNA expression in our 2xCGA, 4xCGA, and 6xCGA strains and found that RNA expression was increased in our 4xCGA and 6xCGA-containing strains but there was no change in the 2xCGA strain (Figure 2.3.4B). Together, these results imply Hel2-mediated RQC and NGD are partially responsible for the observed decrease in protein and RNA expression, respectively, in the wild-type strains. Lastly, we sought to measure the impact of Hel2 on elongation time. A recent review by Meydan and Guydosh proposed two non-mutually exclusive models of Hel2's activity on the stability of ribosome collisions: (1) Hel2 is necessary to rescue stalled ribosomes and Hel2 deletion would result in further buildup of collided ribosomes and (2) Hel2 stabilizes collided ribosomes and Hel2 deletion would result in reduced ribosomal pausing (Meydan and Guydosh 2020). To assess the effect of Hel2 on ribosome pausing and distinguish between these two models, we compared the elongation time of our control, 4xCGA, and 6xCGA strains between WT and ΔHel2 backgrounds and found no significance in our control strain but a decrease in overall elongation time in our 4xCGA and 6xCGA strains when expressed in a ΔHel2 background (Figure 2.3.4C). This suggests that Hel2 functions to slow down elongation in our CGA-containing strains and is consistent with the second proposed model in which Hel2 stabilizes collided ribosomes.

2.3.3 Synonymous substitution to nonoptimal codons negatively impacts gene expression

Next, we asked how distributed slowdowns of non-optimal codons impact gene expression and elongation time. To study the impact of distributed non-optimal codons, we used our optYFP-nLuc construct and synonymously substituted the first 20 of 21 leucines for a nonoptimal leucine variant (Figure 2.3.5). First, we wanted to determine the impact of these synonymous substitutions on overall elongation time. We measured the elongation time in each of our strains and compared it to the optimized strain to determine the elongation time delay associated with each synonymous substitution (Figure 2.3.6A). We found that substitution of the optimal leucine codon TTG for the nonoptimal codons CTC and CTT resulted in a significant delay in elongation time of approximately 0.5 and 2.5 minutes, respectively. Due to the statistically significant differences in elongation time, we selected both the CTC and CTT-containing constructs for further study. Next, we measured the impact of codon substitution on protein and RNA expression (Figures 2.3.6B and 2.3.6C). As compared to the optimized control, we determined that substitution to the CTC codon reduced both protein and mRNA expression approximately by 20% and substitution to the CTT codon reduced both protein and mRNA expression by 50%. This was distinct from the RQC inducing acute stalls that decreased protein production more substantially than they did mRNA expression.

We sought to determine whether the increase in elongation time and decrease in protein expression observed was either contributed equally by each non-optimal codon or the specific placement of non-optimal codons in the YFP ORF. To assess this, we

created a set of chimeric reporters in which the first 10 leucines in the YFP ORF were either optimal or nonoptimal followed by the next 10 leucines of the opposite optimality (Figure 2.3.5). We hypothesized that if each codon contributed equally to elongation time, the elongation time delay of our chimeric constructs would be half of the delay between optYFP and YFP[CTT]. Instead, we found that both the elongation delay and protein expression of our chimeric YFP[CTT/TTG] closely resembled YFP[CTT] and that our chimeric YFP[TTG/CTT] closely resembled YFP[TTG] (Figures 2.3.6D and 2.3.6E, left panels). This provides evidence that substitution of leucines to a nonoptimal variant in the 5' half of the YFP ORF is sufficient to drive protein expression and elongation time outcomes.

A recent study by Chu and colleagues showed that poor codons in the 5' region of a transcript could negatively affect translation initiation through ribosome buildup preventing initiation from occurring, thereby reducing overall translational output (Chu et al. 2014, Hanson and Coller 2018). To test if the observed decrease in protein expression was a result of interference with initiation, we inserted a yeast-optimized miRFP (315 amino acids) upstream of our optYFP-nLuc and YFP[CTT]-nLuc constructs. We hypothesized that if initiation was negatively impacted by ribosome buildup, addition of a long yeast-optimized ORF upstream of the nonoptimal YFP[CTT] would rescue protein expression as compared to the optimal construct. Instead, we found that a statistically significant difference remained between the optimal and CTT-containing nonoptimal constructs (Figure 2.3.6E, right panel). Furthermore, we assessed the impact on elongation time and found that elongation time was not rescued back to WT levels and the magnitude of delay is similar to the YFP[CTT] construct (Figure 2.3.6D,

right panel). This suggests that the decrease in protein expression in YFP[TTG] is a result of the specific placement of the nonoptimal CTT codons within the 5’ half of the YFP ORF.

2.3.4 Gene expression in nonoptimal codon constructs is affected by deletion of Dhh1 but not Hel2

Lastly, we wanted to investigate if Hel2 or other translation sensors were responsible for the negative impacts on gene expression in our nonoptimal codon substituted constructs. Of particular interest was the RNA binding protein Dhh1, a conserved DEAD-box helicase previously shown to have roles in mRNA decapping and translational repression (Carroll et al. 2011, Coller et al. 2001, Fischer and Weis 2002, Tseng-Rogenski et al. 2003). Importantly, it has been shown to bind preferentially to mRNA with low codon optimality and has been proposed to slow down ribosome movement (Sweet et al. 2012, Radhakrishnan et al. 2016). We hypothesized that the negative impacts on gene expression observed in YFP[CTC] and YFP[CTT] compared to the optYFP control may be a result of either Hel2 or Dhh1 influence. To test this, we transformed our optYFP, YFP[CTC], and YFP[CTT] constructs into either a ΔDhh1 or ΔHel2 strain.

First, we assessed the impact of protein expression on our constructs in a ΔDhh1 or ΔHel2 strain deletion background (Figure 2.3.7A). Based on Dhh1’s role in mediating translation repression of transcripts enriched in nonoptimal codons, we expected to see no impact in optYFP and a rescue of protein expression in YFP[CTC] and YFP[CTT]. Instead, we found that deletion of Dhh1 slightly increased protein expression in our

optYFP construct but decreased protein expression in our YFP[CTC] construct. Surprisingly, we found that Hel2 deletion had no statistically significant effect on protein expression in any of our constructs. This suggests that the drop in protein expression seen in the nonoptimal constructs was not due to a Hel2-mediated mechanism and is distinct from our acute CGA-containing constructs. Next, we examined the effect of Dhh1 on mRNA expression by comparing WT and ΔDhh1 mRNA levels (Figure 2.3.7B). We found that deletion of Dhh1 decreased mRNA expression in our YFP[CTC] construct but had no statistically significant difference in the other constructs. The negative impact of Dhh1 deletion in our YFP[CTC] construct was of similar magnitude in protein and mRNA. This suggests that Dhh1 increases mRNA levels in our YFP[CTC] construct, which leads to increased protein expression.

Lastly, wanted to determine the impact of ΔDhh1 and ΔHel2 deletion backgrounds on elongation time in our substituted leucine constructs. We measured elongation delay by comparing the elongation times of our constructs in each deletion strain to WT (Figure 2.3.7C). We found that deletion of Dhh1 increased elongation delay in our optYFP and YFP[CTC] strains, suggesting that Dhh1 functions to speed up elongation in these constructs. We found no statistically significant difference in elongation times in our ΔHel2 deletion strains. This is consistent with the ΔHel2 protein expression data and supports the idea that a non-Hel2-mediated pathway is responsible for the negative impact on gene expression in our substituted leucine constructs.

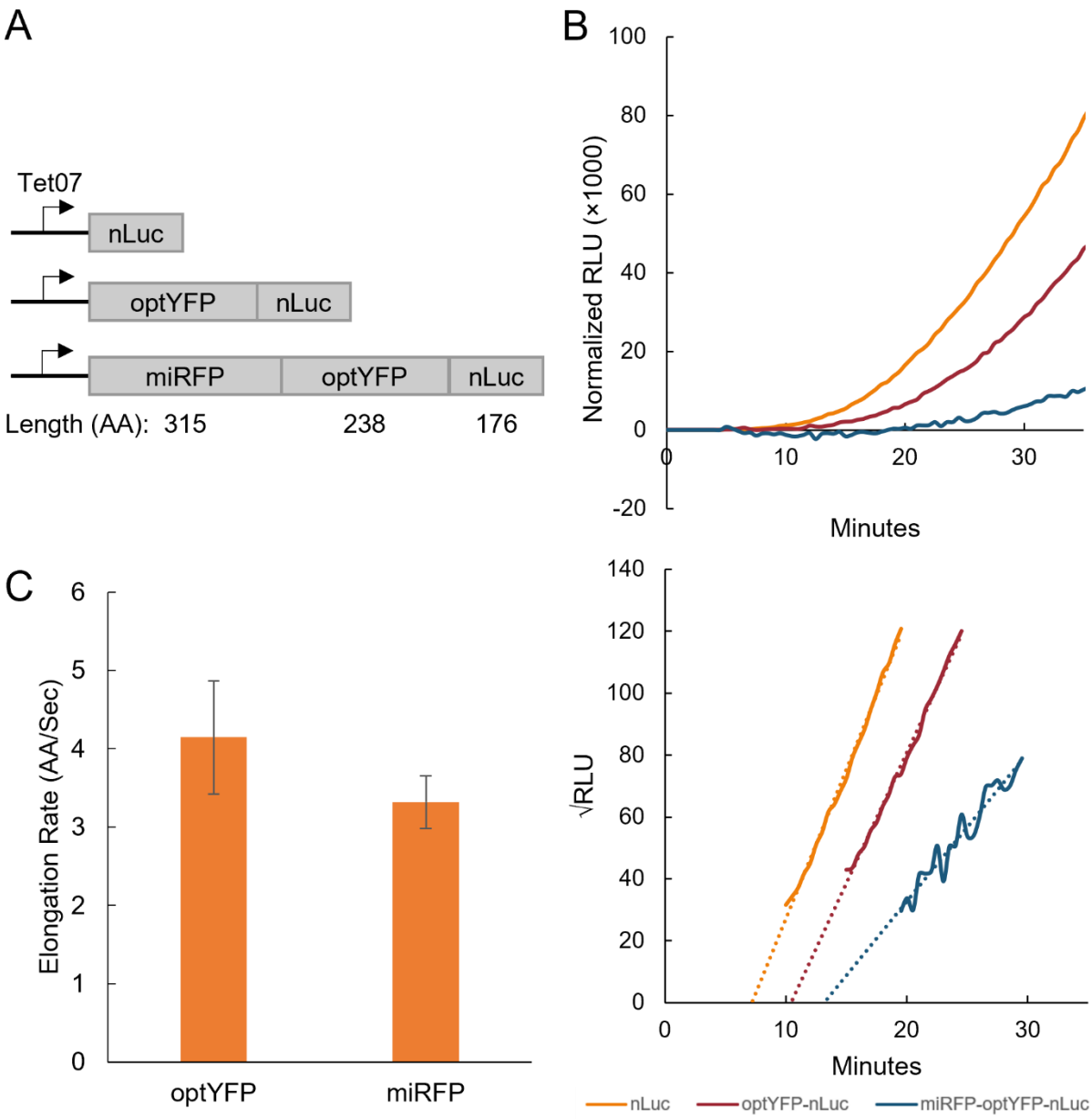

Figure 2.3.1 Assay validation via elongation rate measurements. A: Diagram of yeast-optimized constructs of various lengths. Optimized YFP (optYFP) or both optYFP and optimized miRFP (miRFP) are set upstream of a nanoluciferase (nLuc) reporter. Constructs are expressed from an inducible Tet07 promoter. B: (Top) Representative assay data of relative light units (RLU) of each construct over time normalized to OD600. (Bottom) Schleif plot and associated trendlines of the top graph. C: Calculated elongation rate measurements of optYFP (n=9) and miRFP (n=4) ORFs. Error bars indicate SEM.

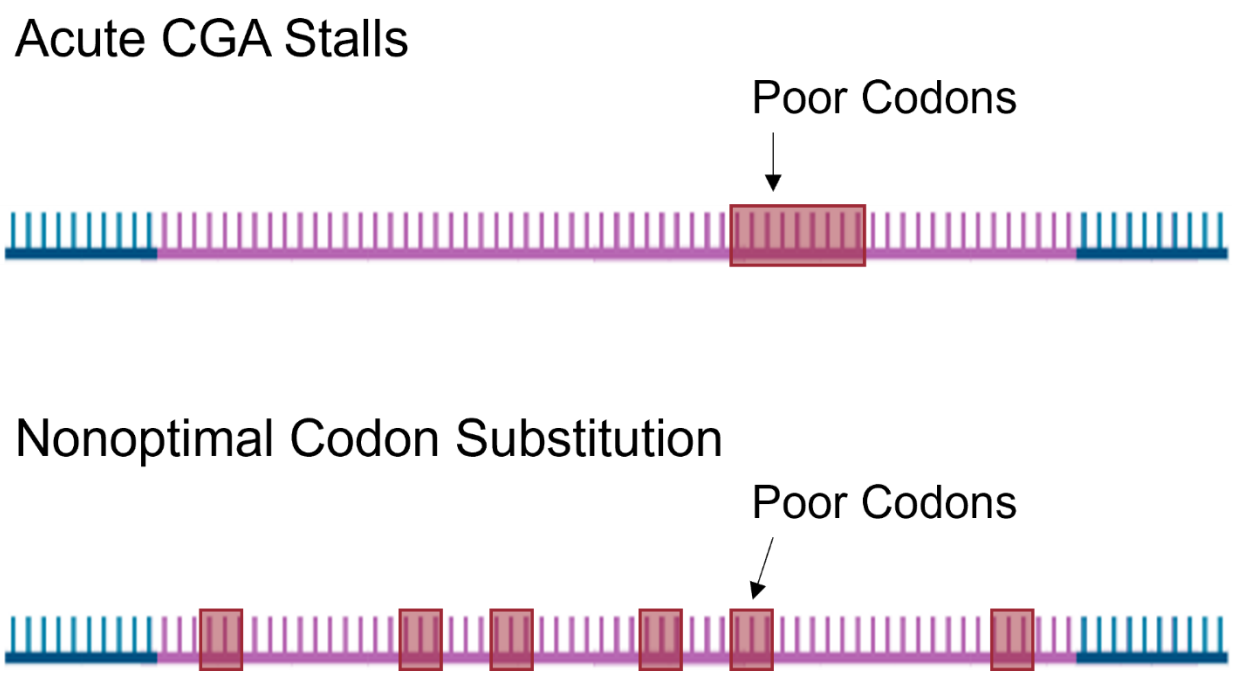

Figure 2.3.2 Diagram of acute CGA stalls and nonoptimal codon substitution. (Top) Nonoptimal CGA codons are inserted internally in an ORF resulting in a strong, localized stall. (Bottom) Optimal TTG leucine codons are synonymously substituted to nonoptimal leucine codon variants, resulting in a general slowdown of elongation.

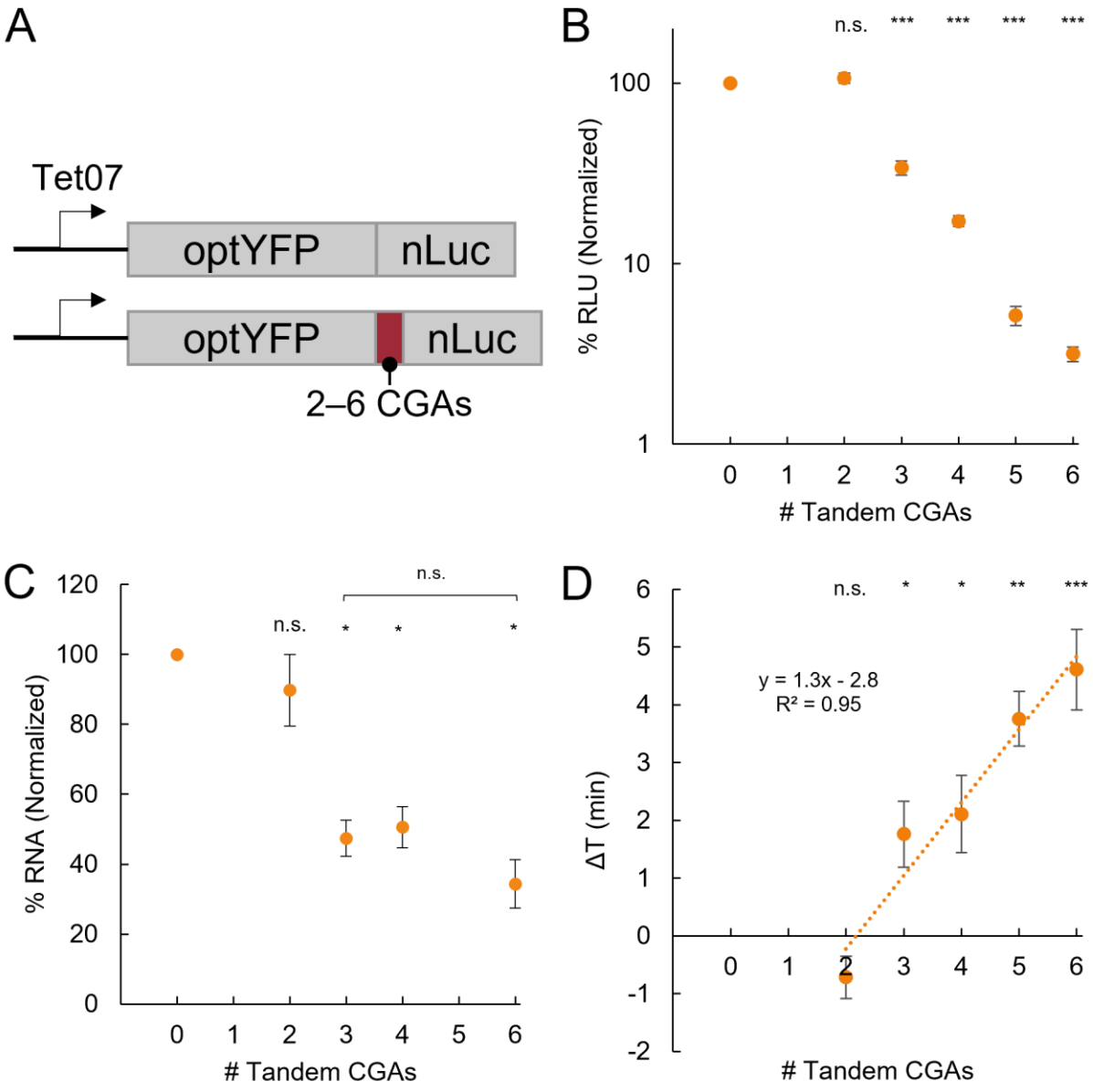

Figure 2.3.3 CGA-derived acute stalls negatively impact gene expression in a dose-dependent manner. A: Diagram of optimal and CGA-containing constructs. Between 2 and 6 CGAs are inserted between the optYFP and nLuc ORFs. B: Protein expression of CGA constructs at T=60 min normalized to optimized control (2xCGA n=10, 3xCGA n=8, 4xCGA n=10, 5xCGA n=5, 6xCGA n=10). C: mRNA expression of CGA constructs at T=60 min normalized to optimized control. (n=3). C: Elongation delay of CGA-containing constructs compared to optimized control. (n=3). All error bars indicate SEM. All statistical significances were calculated for each construct using two-tailed paired Student's t-Test against optYFP control.

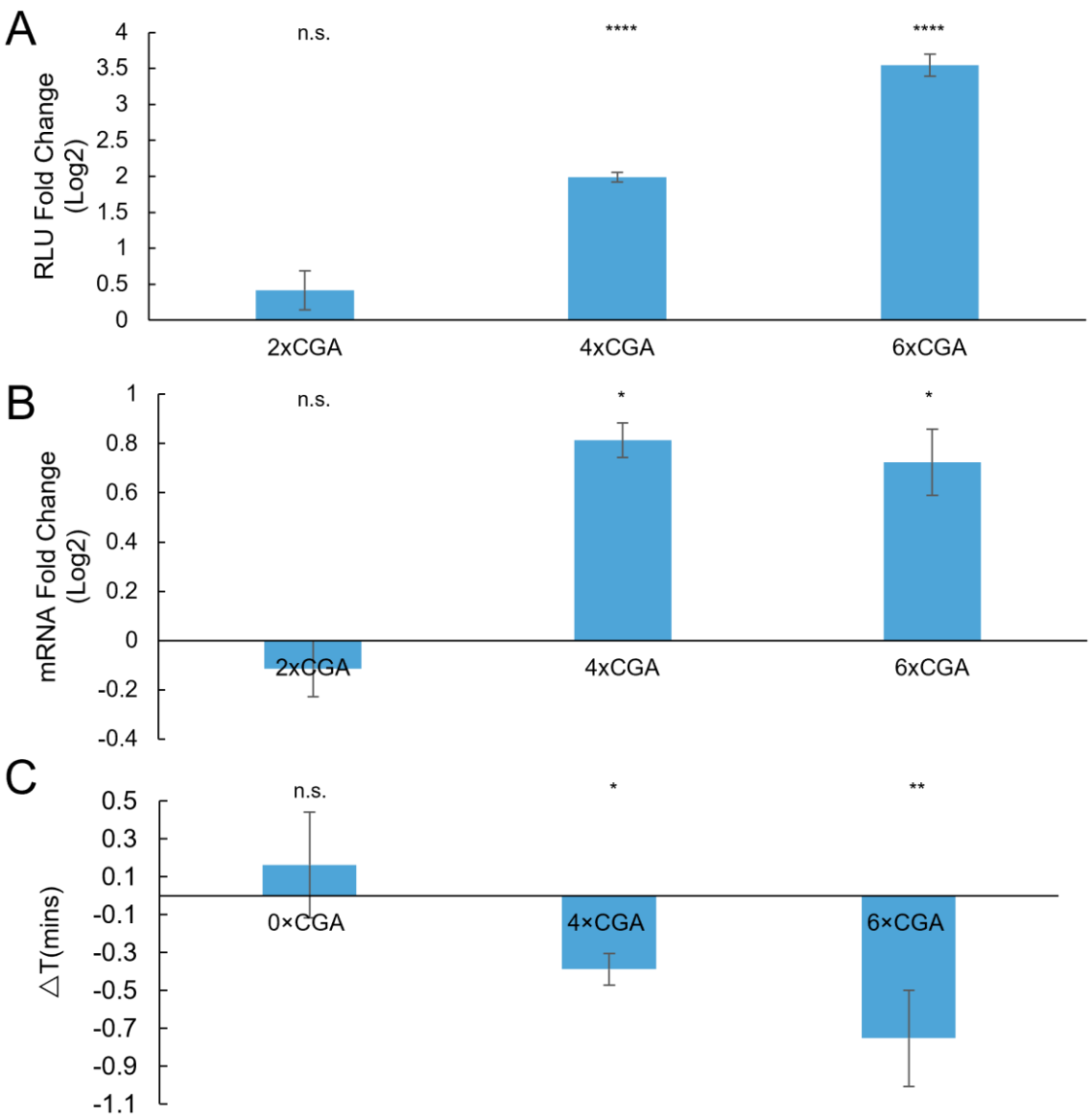

Figure 2.3.4 Hel2 deletion rescues protein expression, mRNA expression, and elongation time. A: Protein expression fold change of CGA constructs in a ΔHel2 vs WT background (2xCGA n=2, 4xCGA n=7, 6xCGA n=7). B: mRNA expression fold change of CGA constructs in a ΔHel2 vs WT background (n = 3). C: Elongation delay of CGA constructs in a ΔHel2 vs WT background (n = 3). All error bars indicate SEM. All statistical significances were calculated for each construct using two-tailed paired Student's t-Test against WT control.

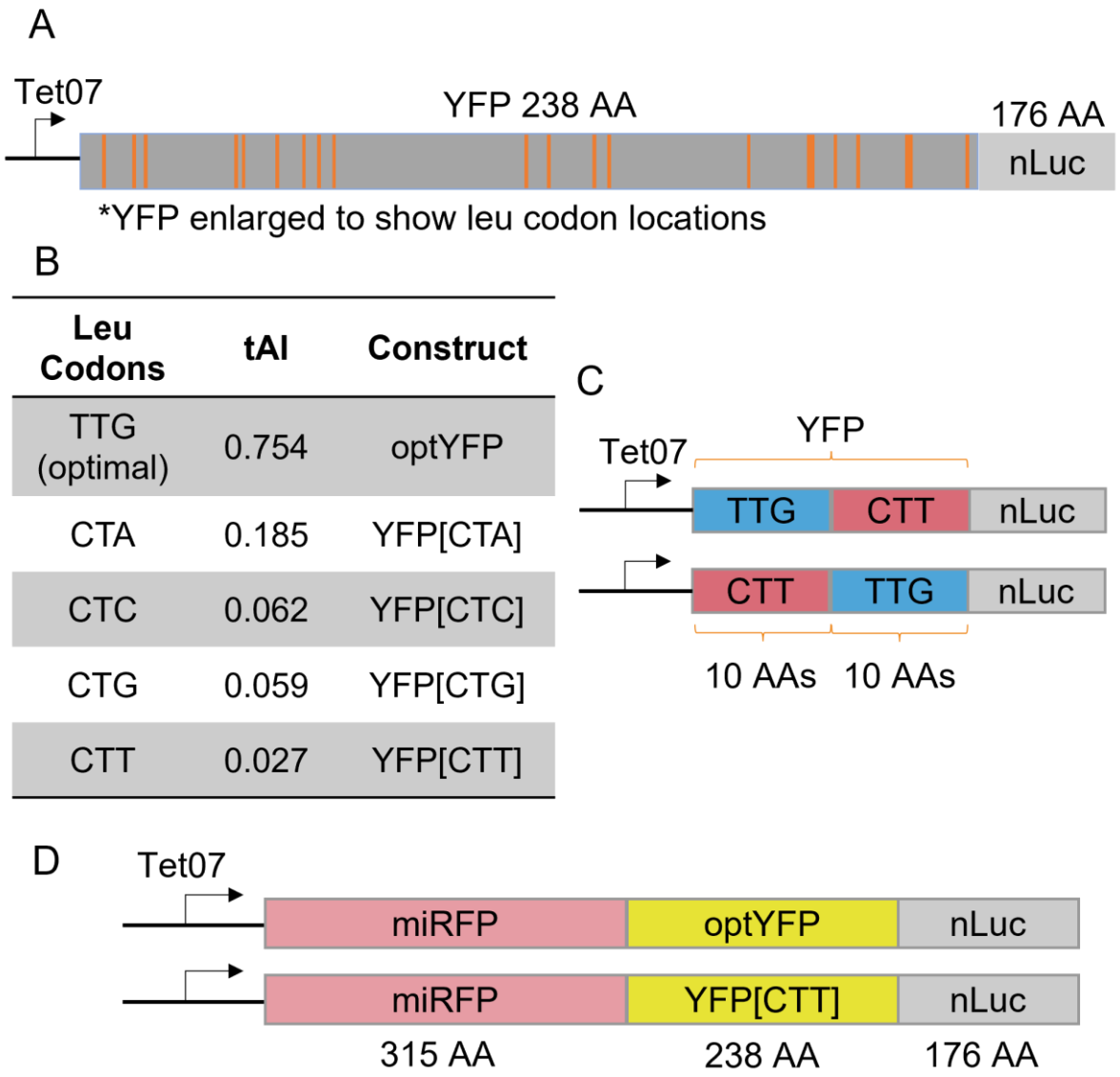

Leu Codons	tAI	Construct
TTG (optimal)	0.754	optYFP
CTA	0.185	YFP[CTA]
CTC	0.062	YFP[CTC]
CTG	0.059	YFP[CTG]
CTT	0.027	YFP[CTT]

Figure 2.3.5 Diagrams of synonymous substituted leucine constructs. A: Diagram of synonymously substituted leucine constructs. Yeast-optimized YFP (optYFP) contains 21 leucine codons which are marked in orange. The first 20 leucine codons are substituted for a nonoptimal leucine variant. Constructs contain an Tet07 inducible promoter. B: Table of leucine codons used in this study. The optimal TTG codon is present in the optYFP control. Other constructs contain a nonoptimal leucine variant which is denoted in brackets. The tRNA Adaptation Index (tAI) is a metric that represents codon optimality and ranges from 0 (most nonoptimal) to 1 (most optimal). C: Diagram of chimeric leucine constructs. The first 10 leucines are either optimal (TTG) or nonoptimal (CTT) followed by 10 leucines of the opposite optimality. Constructs contain a Tet07 inducible promoter. D: Diagram of miRFP-containing constructs. A yeast-optimized miRFP ORF is placed upstream of either optYFP-nLuc or YFP[CTT]-nLuc constructs. Addition of the optimized upstream miRFP is hypothesized to mitigate the effect of ribosome buildup interfering with initiation. Constructs contain a Tet07 inducible promoter.

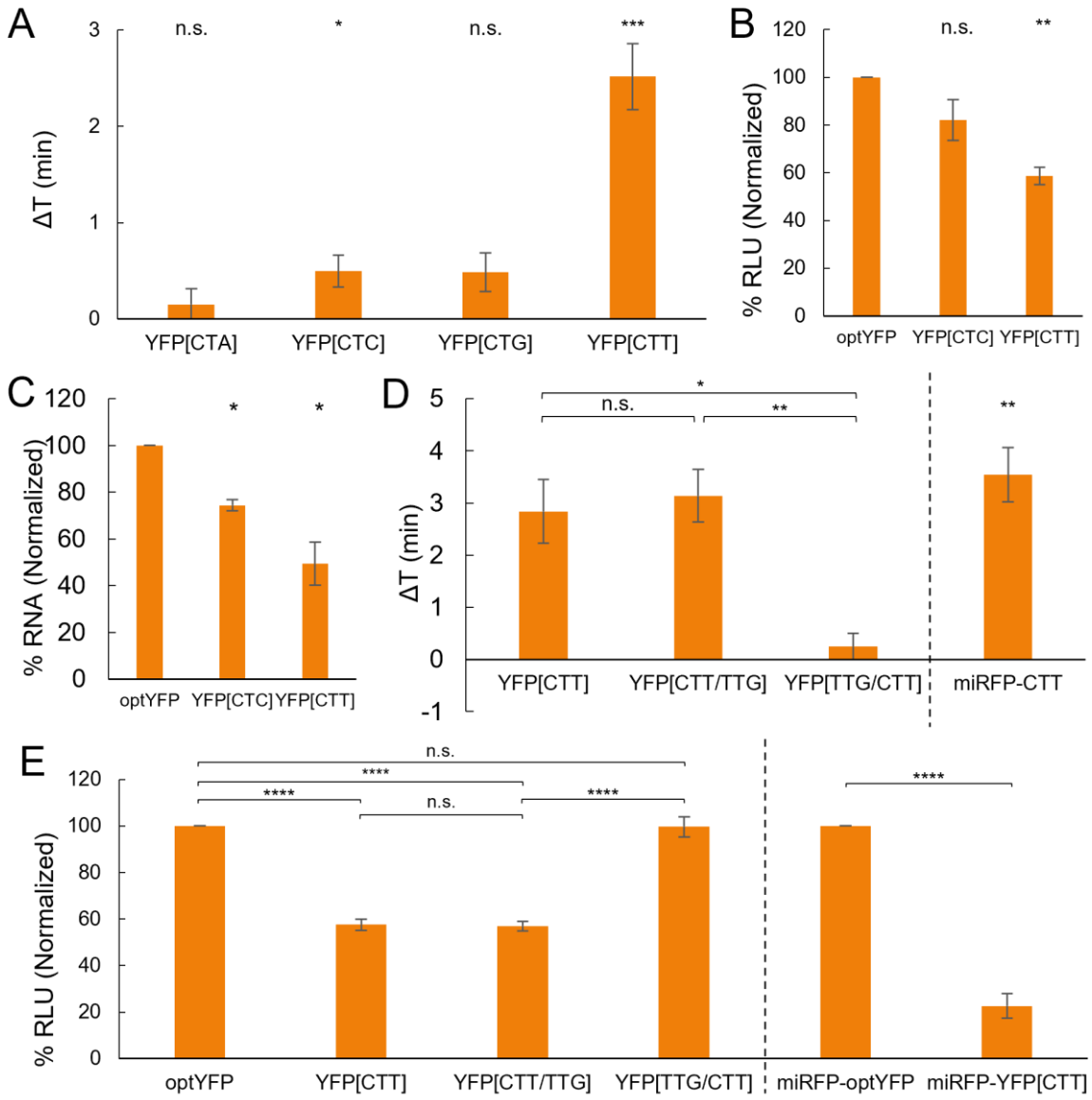

Figure 2.3.6 Distributed stalls in the YFP ORF decrease protein expression, mRNA expression, and delays elongation time. A: Elongation delay of distributed stall constructs compared to optYFP (CTA n=6, CTC n=6, CTG n=5, CTT n=7). The first 20 out of 21 total optimal TTG leucine codons in optYFP are synonymously substituted to a nonoptimal codon specified in brackets. B: Protein expression of distributed stall constructs normalized to optYFP control (n=4). C: mRNA expression of distributed stall constructs normalized to optYFP control (n=3). D: (Left) Elongation delay measurements of chimeric constructs normalized to optYFP control (n=9). (Right) Elongation delay measurements of miRFP-YFP[CTT] normalized to miRFP-optYFP control (n=6). E: (Left) Protein expression chimeric constructs normalized to optYFP control (n=5). (Right) Protein expression of miRFP-YFP[CTT] normalized to miRFP-optYFP control (n=6). All error bars indicate SEM. All statistical significances were calculated for each construct using two-tailed paired Student's t-Test against optYFP control unless otherwise specified.

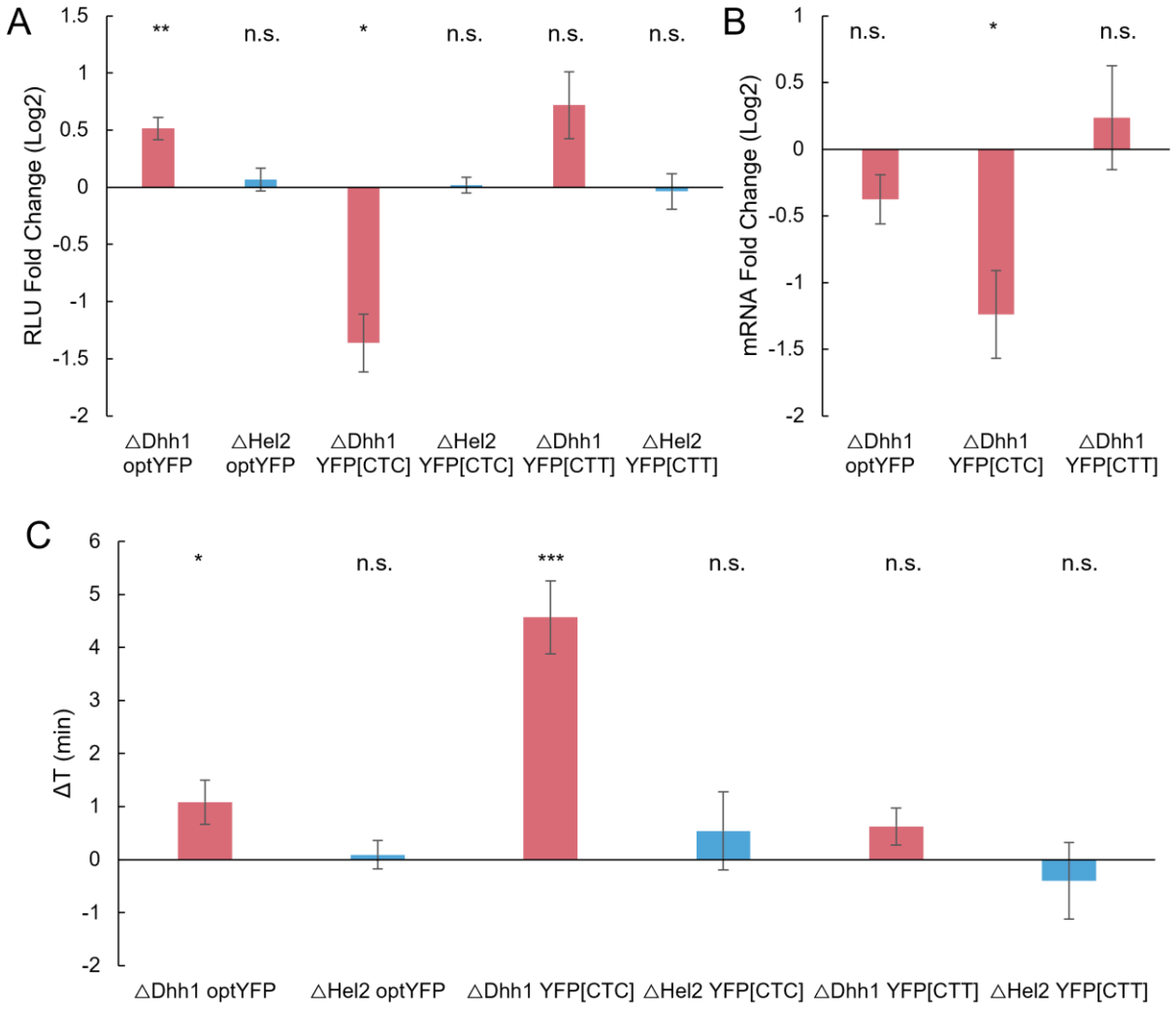

Figure 2.3.7 Dhh1 deletion, but not Hel2 deletion, affects gene expression in substitution constructs. A: Protein expression of distributed stall constructs in ΔDhh1 or ΔHel2 background vs WT (n=5, 4, 5, 6, 7, and 3 from left to right). B: mRNA expression fold change of distributed stall constructs in a ΔDhh1 vs WT background (n = 5, 5, and 7 from left to right). C: Elongation delay of distributed stall constructs in ΔDhh1 or ΔHel2 background vs WT (n= 19, 4, 18, 6, 9, and 5 from left to right). All error bars indicate SEM. All statistical significances were calculated for each construct using two-tailed paired Student's t-Test against WT control.

2.4 Discussion

Ribosome stalling and the connected quality control pathways are important for recognizing faulty and damaged mRNAs, yet quantitative measurements of how these stalls impact translation duration have been lacking. In this study, we developed a reporter assay to quantify the *in vivo* elongation time of various constructs containing stalling sequences in *S. cerevisiae*. Using CGA stalling reporters we find that total elongation time increases in a dose-dependent manner corresponding with the number of tandem CGA repeats while protein expression decreases logarithmically with increasing CGA repeats. Strikingly, we find that mRNA levels stabilize upon reaching a specific stall length, suggesting that the stall-activated NGD pathway reaches a maximum decay rate at 3x CGA. Interestingly the ~50% reduction in mRNA levels is very similar to the mRNA reduction seen from a completely independently designed reporter containing 12xCGA (Veltri et al 2021), further supporting NGD may be saturated at relatively shorter translational stalls.

From our synonymous leucine substitution constructs, we find that the nonoptimal codon CTT causes substantial delays in elongation time on the order of minutes. The elongation delay of ~ 150s for the CTT reporter is very similar to the elongation delay for our 4xCGA stalling reporter. Yet these two reporters behave very differently as the decrease in protein expression due to CTT could be explained completely by decreased mRNA levels, while the 4xCGA decreased protein levels to an even larger extent then the ~50% decrease in mRNA levels. This pointed to the induction of RQC, which reduces protein expression on the CGA stalls through ribosome rescue. Further supporting this induction of RQC on CGA stalls but not CTT

stalls, deletion of the RQC factor could partially rescue the mRNA levels and protein production of CGA stalls, yet it had no significant effect on protein production and elongation times due to non-optimal CTT codons. These data point to further differentiation of ribosome stalling beyond just stall duration timing.

While 20 synonymous Leu codons were changed to poor CTT codons, not all non-optimal codons contribute equally to the elongation slowdown. Instead, the second set of 10 Leu codons had no measurable effect on elongation or protein production, while the first 10 Leu were sufficient to impact elongation and protein production. This appear to be caused by local sequence effects and not specifically the poor codons being in the 5' end of the ORF, as adding an upstream miRFP ORF was not able to rescue the translation slowdown and reduced protein production. This argues that local sequence context is important for determining the effects of codon optimality on gene expression. This fits with reports showing that specific combinations of codons modulate translation efficiency and mRNA decay (Gamble et al. 2016, Burke et al. 2021).

We found that CGA stalls added ~76s per CGA codon to the translation duration of the reporter after 3xCGAs. This led to an almost 5 minute lengthening of translation duration for a 6xCGA construct. A recent paper by Goldman and colleagues examined ribosomal clearance times on mRNA containing difficult-to-translate polyA-containing stretches and found it took approximately 10 and 13 minutes for ribosomes to clear off 50% of transcripts containing poly(A)36 and poly(A)60 stretches, respectively. Their finding on delays lasting on the order of minutes is consistent with our findings and represents an intriguing observation considering that the average half-life of yeast mRNAs is ~10 minutes, suggesting that a significant portion of an mRNA's half-life can

be spent engaged in a ribosomal stall (Chan et al. 2018). Furthermore, we were surprised that substitution of a relatively small percentage of codons (20 out of 176 coding codons in YFP; approximately 11%) was sufficient to increase elongation time by minutes. Considering ribosome pauses and their role in co-translational protein folding, recognition of localization signals on nascent proteins, and overall protein output, inclusion of these significantly-slowing codons may be a useful mechanism to add an extended pause on the order of seconds when necessary during elongation with a single codon.

Previous research suggests that Hel2 senses stalled ribosomes and mediates surveillance pathways such as RQC and NGD. Throughout RQC and NGD pathways, nascent peptides and detrimental mRNA will be degraded respectively to help cells survive. Theoretically, within a Hel2-depletion strain, both protein production and mRNA expression will be rescued since we kill RQC and NGD pathways. We found Hel2 deletion rescues mRNA level back to WT levels, while partially rescuing protein expression, which proposes that protein production is influenced by multifaceted ways.

It is well-confirmed that Hel2 is a necessary factor mediating RQC and NGD pathways however its effects on ribosome stalling have been unclear. Two non-mutually exclusive models have been proposed: first, since Hel2 is needed to promote the rescue of the stalled ribosome in a collision complex, deletion of Hel2 will slow ribosome rescue, resulting in accumulated collided ribosomes, which increases elongation delay; In second model, we propose that Hel2 is able to sense and stabilize stalled ribosomes to prevent further translation. In this scenario, deletion of Hel2 would destabilize collided ribosomes, resulting in rescued elongation and shorter elongation delay. In this paper,

we quantitatively measure the change of elongation delay after Hel2 depletion and find a reduction in the translation duration of CGA stalled sequences. This is distinct from mammalian cells, where depletion of the mammalian homolog of Hel2, ZNF598, causes further delays in the clearing of ribosomes.

It has been previously reported that Dhh1 plays a role in degradation of mRNA enriched in nonoptimal codons. We can then predict that Dhh1 deletion would increase mRNA expression in our nonoptimal codon-substituted constructs. We were surprised to find that Dhh1 deletion instead decreases the expression of the YFP[CTC] construct. As the YFP constructs used in this study are all yeast optimized except for the leucine codons, it is possible that Dhh1 deletion would only be beneficial for mRNAs more enriched in poor codons. Previous work demonstrates a negligible effect of Dhh1 deletion on mRNA half-life for primarily optimal mRNA (Radhakrishnan et al. 2016). The Dhh1 deletion background also presents a slowdown in growth rate compared to the wild type (120 minutes per doubling time versus 90 minutes for the wildtype background). This general slowdown in growth may result in a small slowdown of elongation that, in combination with the slowdown due to CTC codons, results in the YFP[CTC] construct slowing down sufficiently to cause increased ribosome collisions and reductions in mRNA stability independently of direct effects due to the Dhh1 deletion.

Although most studies have investigated Dhh1 with regards to its role in mRNA decay and translational repression, Dhh1 has also been shown to promote the translation of certain mRNAs as well. It has been previously demonstrated that a subset of mRNAs that contain highly-structured 5’UTRs and coding sequences require Dhh1

helicase activity for efficient expression (Jungfleisch et al. 2017). Furthermore, Dhh1 can shift roles in a condition-dependent manner. During nitrogen starvation, Dhh1 is required for the efficient expression of autophagy-related proteins Atg1 and Atg13, but when nutrients are plentiful Dhh1 encourages ATG mRNA degradation (Liu et al. 2019). Overall, this argues that Dhh1 may play context specific roles in translation elongation and may be able to speed up elongation in specific sequence contexts.

2.5 Materials and Methods

Plasmid Preparation and Integration. All plasmids used in this study are listed in Table 2.5.1. Plasmids containing synonymous leucine codon substituted YFP (TTG, CTA, CTC, CTG, and CTT) and a single-copy yeast integrating plasmid containing a pTET07 promoter were provided as a kind gift from Dr. Arvind R. Subramaniam at the Fred Hutchinson Cancer Research Center in Seattle, Washington. Fragments containing pTET07, YFP variants, and yeast-optimized nanoluciferase (Promega Cat. No. N1141) were amplified using PCR and cloned into the *XhoI* and *HindIII*-digested single-copy yeast integrating plasmid using Gibson assembly.

The pAG306-pTet07-YFP[CTT/TTG]-nLuc and pAG306-pTet07-YFP[TTG/CTT]-nLuc split strains were generated by PCR amplification of the entire backbone of the previous pAG306-pTet07-YFP[TTG]-nLuc plasmid beginning at nLuc and ending with pTet07, and PCR amplification of the first (1-377 bp from CDS start) and second (378-714 bp from CDS start) halves of the TTG and CTT YFP variants between the 10th and 11th leucine codons. These fragments were combined using Gibson assembly.

Plasmid variants containing two to six CGA stalls were generated using the aforementioned backbone PCR of the pAG306-pTet07-YFP[TTG] plasmid and a PCR amplified YFP[TTG] fragment containing two to six CGA repeats as a 3' overhang. These fragments were combined using Gibson assembly.

All plasmids were linearized using *NotI* and integrated into yeast by homologous recombination. Integrations were screened by growing transformed yeast on synthetic complete (SC) dropout plates lacking uracil. These were then frozen down for long-term storage in YPD containing 15% v/v glycerol.

Yeast Strains, Growth, and Media. The background yeast strain w303 (EY0690) was used for all experiments. Yeast Dhh1 and Hel2 deletion strains were created by deleting the endogenous Dhh1 and Hel2 loci, respectively, using pRS315 (Addgene Plasmid #3974) and screened by growing transformed yeast on SC dropout plates lacking leucine. Specific oligos used are listed in Table 3.5.2. Yeast strains were frozen down in YPD containing 15% v/v glycerol.

For cells cultured for use in our reporter assay, cells were streaked out from frozen stocks onto YPD Agar plates and grown at 30 °C for two days. These plates were stored at 4 °C for up to one month.

Luciferase-Based Elongation Reporter Assay. Liquid cultures were started from single colonies and allowed to grow overnight at 30 °C with shaking until an approximate OD600 of 0.3-0.5 after which cultures were divided into two tubes. For one of the tubes, 1 µL of a stock solution of anhydrotetracycline (250 µg/mL of ATC dissolved in EtOH) was added per mL of culture. Both tubes were returned to 30 °C with shaking for five to ten minutes. 90 µL of each culture was added to a 96-well white flat-

bottom plate (Grainger) and to each well, 10 uL of furimazine (10 mM furimazine stock solution dissolved in DMSO diluted 1:200 in YPD), was added. Immediately after sample loading, the plate was placed in a 30 °C prewarmed Tecan Infinite® 200 PRO plate reader. The following program was used and luminescence measurements were taken every 30 or 60 seconds: (1) Kinetic Cycle: [Cycle Duration: 60 minutes, Kinetic Interval: 30 or 60 seconds], (2) Shaking: [Duration: 3 seconds, Mode: Orbital, Amplitude 2 mm], (3) Luminescence: [Attenuation: Automatic, Integration Time: 1000 ms, Settle Time: 0 ms].

Schleif Plot and Elongation Delay Measurements. The Schleif Plot methodology was adapted from Schleif, R., et al. (1973) and slightly modified to assume a non-constant basal expression protein level. For each sample, ATC-induced protein expression was calculated by subtracting the samples lacking ATC (-ATC) from the corresponding samples with ATC (+ATC) across all measured timepoints. Samples were then normalized to an OD600 of 1.0 by dividing their protein expression over time by their respective ODs. All values were then subtracted by the average RLU of the first 5 minutes to subtract background. Then, the square root of each value was calculated and plotted against time. Values that produced an error due to the square root of a negative value were set as “N/A” and avoided in our analysis. From this Schleif plot, we identified regions of linearity across our samples and selected a 10-15 minute window for analysis. Ideally, these regions of linearity are parallel between each sample and contain a minimal amount of noise. For each time window, we created a trendline and calculated the X-intercept of the trendline which represented the calculated elongation time of the sample. The calculated elongation time of the samples in a single assay

were then compared to a control to determine elongation delay. These elongation delay measurements were then compared across assays and aggregated to determine the average elongation delay associated with the specific construct.

RNA Extraction and Real Time qPCR. Yeast pellets were collected from samples 60-minutes post-ATC addition by spinning 1-1.5 mL of liquid culture at 3000 *x g* for 2 minutes and discarding the supernatant. These yeast pellets were then flash frozen in liquid nitrogen and stored at -80 °C until RNA extraction. RNA was extracted from yeast pellets using the MasterPure™ Yeast RNA Purification Kit (Lucigen Cat. No. MPY03100) according to the manufacturer's instructions. RNA quality and concentration was assessed using a Nanodrop.

RNA samples were subjected to DNase digestion using RQ1 RNase-free DNase (Promega) according to the manufacturer’s instructions. cDNA was prepared from equal amounts of RNA from each sample using Protoscript II Reverse Transcriptase (New England Biolabs Cat. No. M0368X) and an oligo dT(18) primer according to the manufacturer’s instructions. RT-qPCR was done using a home-brew recipe with SYBR Green at a final concentration of 0.5X (Thermo Fisher S7564). Primers specific for nanoluciferase and actin are described in Table 3.5.2. mRNA levels were normalized to ACT1 abundance and fold change was calculated by a standard Ct analysis.

Table 3.5.1 List of plasmids used in elongation study

Construct Name	Identifier	Plasmid
nLuc	ZP427	pAG306-pTet-nLuc
optYFP	ZP436	pAG306-pTet-YFP[TTG]-nLuc
2xCGA	ZP464	pAG306-pTet-YFP[TTG]-2xCGA-nLuc
3xCGA	ZP486	pAG306-pTet-YFP[TTG]-3xCGA-nLuc
4xCGA	ZP465	pAG306-pTet-YFP[TTG]-4xCGA-nLuc
5xCGA	ZP487	pAG306-pTet-YFP[TTG]-5xCGA-nLuc
6xCGA	ZP466	pAG306-pTet-YFP[TTG]-6xCGA-nLuc
YFP[CTA]	ZP432	pAG306-pTet-YFP[CTA]-nLuc
YFP[CTC]	ZP433	pAG306-pTet-YFP[CTC]-nLuc
YFP[CTT]	ZP434	pAG306-pTet-YFP[CTT]-nLuc
YFP[CTG]	ZP435	pAG306-pTet-YFP[CTG]-nLuc
YFP[CTT/TTG]	ZP513	pAG306-pTet-splitYFP[CTT/TTG]-nLuc
YFP[TTG/CTT]	ZP515	pAG306-pTet-splitYFP[TTG/CTT]-nLuc
miRFP-optYFP	ZP531	pAG306-pTet-miRFP-YFP[TTG]-nLuc
miRFP-YFP[CTT]	ZP530	pAG306-pTet-miRFP-YFP[CTT]-nLuc

Table 3.5.2 List of primers used in elongation study

Primer Name	Identifier	Sequence
Actin Fwd	ZO83 qAct1_F	CTGCCGGTATTGACCAAACT
Actin Rev	ZO84 qAct1_R	CGGTGATTTCCTTTTGCATT
nLuc Fwd	ZO553 q_nLuc_F	TGGTGATCAAATGGGTCAAA
nLuc Rev	ZO544 q_nLuc_R	CCTTCATAAGGACGACCAAA
Hel2 Deletion Fwd	ZO1186 Hel2prF	CTAATGCTATTGTCAGTTACAGGTTAGAAATA TATTTCCAA CGG ATC CCC GGG TTA ATT AA
Hel2 Deletion Rev	ZO1187 Hel2prR	CGAAAAAATAGTGGCTATACTTCTTTTCAA GAATTAGG GAA TTC GAG CTC GTT TAA AC
Dhh1 Deletion Fwd	ZO113 Dhh1prF	ATCCCAGGCCTAAAATACGACAAGAAAGAAA ATAGTAGTA CGG ATC CCC GGG TTA ATT AA
Dhh1 Deletion Rev	ZO114 Dhh1prR	GCGTATCTCACCACAGTAGTTATTTTTTCTT AGATATTCT GAA TTC GAG CTC GTT TAA AC

2.6 Acknowledgments

Chapter 2, in full, is currently being prepared for submission for publication of the material: Harjono, V, Hou, W, Harvey, AT, Subramaniam, AR, and Zid, BM. Quantification of elongation stalls and impact on gene expression in yeast. The dissertation author is the primary author of this material.

2.7 References

1. Bosco, D. A. (2018). Translation dysregulation in neurodegenerative disorders. *Proceedings of the National Academy of Sciences*, *115*(51), 12842-12844.

2. Wang, E. T., Taliaferro, J. M., Lee, J. A., Sudhakaran, I. P., Rossoll, W., Gross, C., Moss, K. R., & Bassell, G. J. (2016). Dysregulation of mRNA localization and translation in genetic disease. *Journal of Neuroscience*, *36*(45), 11418-11426.

3. Sonenberg, N., & Hinnebusch, A. G. (2009). Regulation of translation initiation in eukaryotes: mechanisms and biological targets. *Cell*, *136*(4), 731-745.

4. Shah, P., Ding, Y., Niemczyk, M., Kudla, G., & Plotkin, J. B. (2013). Rate-limiting steps in yeast protein translation. *Cell*, *153*(7), 1589-1601.

5. Pechmann, S., & Frydman, J. (2013). Evolutionary conservation of codon optimality reveals hidden signatures of cotranslational folding. *Nature structural & molecular biology*, *20*(2), 237-243.

6. Spencer, P. S., Siller, E., Anderson, J. F., & Barral, J. M. (2012). Silent substitutions predictably alter translation elongation rates and protein folding efficiencies. *Journal of molecular biology*, *422*(3), 328-335.

7. Yu, C. H., Dang, Y., Zhou, Z., Wu, C., Zhao, F., Sachs, M. S., & Liu, Y. (2015). Codon usage influences the local rate of translation elongation to regulate co-translational protein folding. *Molecular cell*, *59*(5), 744-754.

8. Zhao, T., Chen, Y. M., Li, Y., Wang, J., Chen, S., Gao, N., & Qian, W. (2021). Disome-seq reveals widespread ribosome collisions that promote cotranslational protein folding. *Genome biology*, *22*(1), 1-35.

9. Hartl, F. U., Bracher, A., & Hayer-Hartl, M. (2011). Molecular chaperones in protein folding and proteostasis. *Nature*, *475*(7356), 324-332.

10. Tsuboi, T., Viana, M. P., Xu, F., Yu, J., Chanchani, R., Arceo, X. G., Tutucci, E., Choi, J., Chen, Y. S., Singer, R. H., Rafelski, S. M., & Zid, B. M. (2020). Mitochondrial volume fraction and translation duration impact mitochondrial mRNA localization and protein synthesis. *Elife*, *9*, e57814.

11. Alamo, M. D., Hogan, D. J., Pechmann, S., Albanese, V., Brown, P. O., & Frydman, J. (2011). Defining the specificity of cotranslationally acting chaperones by systematic analysis of mRNAs associated with ribosome-nascent chain complexes. *PLoS biology*, *9*(7), e1001100.

12. Ogg, S. C., & Walter, P. (1995). SRP samples nascent chains for the presenceof signal sequences by interacting with ribosomes at a discrete step during translation elongation. *Cell*, *81*(7), 1075-1084.

13. Mason, N., Ciufo, L. F., & Brown, J. D. (2000). Elongation arrest is a physiologically important function of signal recognition particle. *The EMBO journal*, *19*(15), 4164-4174.

14. Zhao, T., Chen, Y. M., Li, Y., Wang, J., Chen, S., Gao, N., & Qian, W. (2021). Disome-seq reveals widespread ribosome collisions that promote cotranslational protein folding. *Genome biology*, *22*(1), 1-35.

15. Arpat, A. B., Liechti, A., De Matos, M., Dreos, R., Janich, P., & Gatfield, D. (2020). Transcriptome-wide sites of collided ribosomes reveal principles of translational pausing. *Genome research*, *30*(7), 985-999.

16. Han, P., Shichino, Y., Schneider-Poetsch, T., Mito, M., Hashimoto, S., Udagawa, T., Kohno, K., Yoshida, M., Mishima, Y., Inada, T., & Iwasaki, S. (2020). Genome-wide survey of ribosome collision. *Cell reports*, *31*(5), 107610.

17. Buskirk, A. R., & Green, R. (2017). Ribosome pausing, arrest and rescue in bacteria and eukaryotes. *Philosophical Transactions of the Royal Society B: Biological Sciences*, *372*(1716), 20160183.

18. Yip, M. C., & Shao, S. (2021). Detecting and Rescuing Stalled Ribosomes. *Trends in Biochemical Sciences*.

19. Joazeiro, C. A. (2017). Ribosomal stalling during translation: providing substrates for ribosome-associated protein quality control. *Annual review of cell and developmental biology*, *33*, 343-368.

20. Ikeuchi, K., Tesina, P., Matsuo, Y., Sugiyama, T., Cheng, J., Saeki, Y., Tanaka, K., Becker, T., Beckmann, R. & Inada, T. (2019). Collided ribosomes form a unique structural interface to induce Hel2-driven quality control pathways. *The EMBO journal*, *38*(5), e100276.

21. D'Orazio, K. N., Wu, C. C. C., Sinha, N., Loll-Krippleber, R., Brown, G. W., & Green, R. (2019). The endonuclease Cue2 cleaves mRNAs at stalled ribosomes during No Go Decay. *Elife*, *8*, e49117.

22. Navickas, A., Chamois, S., Saint-Fort, R., Henri, J., Torchet, C., & Benard, L. (2020). No-Go Decay mRNA cleavage in the ribosome exit tunnel produces 5′-OH ends phosphorylated by Trl1. *Nature communications*, *11*(1), 1-11.

23. Meydan, S., & Guydosh, N. R. (2020). A cellular handbook for collided ribosomes: surveillance pathways and collision types. *Current genetics*, 1-8.

24. Presnyak, V., Alhusaini, N., Chen, Y. H., Martin, S., Morris, N., Kline, N., Olson, S., Weinberg, D., Baker, K. E., Graveley, B. R., & Coller, J. (2015). Codon optimality is a major determinant of mRNA stability. *Cell*, *160*(6), 1111-1124.

25. Reis, M. D., Savva, R., & Wernisch, L. (2004). Solving the riddle of codon usage preferences: a test for translational selection. *Nucleic acids research*, *32*(17), 5036-5044.

26. Gardin, J., Yeasmin, R., Yurovsky, A., Cai, Y., Skiena, S., & Futcher, B. (2014). Measurement of average decoding rates of the 61 sense codons in vivo. *Elife*, *3*, e03735.

27. Pechmann, S., Willmund, F., & Frydman, J. (2013). The ribosome as a hub for protein quality control. *Molecular cell*, *49*(3), 411-421.

28. Radhakrishnan, A., Chen, Y. H., Martin, S., Alhusaini, N., Green, R., & Coller, J. (2016). The DEAD-box protein Dhh1p couples mRNA decay and translation by monitoring codon optimality. *Cell*, *167*(1), 122-132.

29. Harigaya, Y., & Parker, R. (2016). Codon optimality and mRNA decay. *Cell research*, *26*(12), 1269-1270.

30. Hanson, G., & Coller, J. (2018). Codon optimality, bias and usage in translation and mRNA decay. *Nature reviews Molecular cell biology*, *19*(1), 20-30.

31. Ingolia, N. T. (2014). Ribosome profiling: new views of translation, from single codons to genome scale. *Nature reviews genetics*, *15*(3), 205-213.

32. Ingolia, N. T., Ghaemmaghami, S., Newman, J. R., & Weissman, J. S. (2009). Genome-wide analysis in vivo of translation with nucleotide resolution using ribosome profiling. *science*, *324*(5924), 218-223.

33. Hussmann, J. A., Patchett, S., Johnson, A., Sawyer, S., & Press, W. H. (2015). Understanding biases in ribosome profiling experiments reveals signatures of translation dynamics in yeast. *PLoS genetics*, *11*(12), e1005732.

34. Gardin, J., Yeasmin, R., Yurovsky, A., Cai, Y., Skiena, S., & Futcher, B. (2014). Measurement of average decoding rates of the 61 sense codons in vivo. *Elife*, *3*, e03735.

35. Weinberg, D. E., Shah, P., Eichhorn, S. W., Hussmann, J. A., Plotkin, J. B., & Bartel, D. P. (2016). Improved ribosome-footprint and mRNA measurements provide insights into dynamics and regulation of yeast translation. *Cell reports*, *14*(7), 1787-1799.

36. Saikia, M., Wang, X., Mao, Y., Wan, J., Pan, T., & Qian, S. B. (2016). Codon optimality controls differential mRNA translation during amino acid starvation. *Rna*, *22*(11), 1719-1727.

37. Chu, D., Barnes, D. J., & Von Der Haar, T. (2011). The role of tRNA and ribosome competition in coupling the expression of different mRNAs in Saccharomyces cerevisiae. *Nucleic acids research*, *39*(15), 6705-6714.

38. Koutmou, K. S., Radhakrishnan, A., & Green, R. (2015). Synthesis at the speed of codons. *Trends in biochemical sciences*, *40*(12), 717-718.

39. Masser, A. E., Kandasamy, G., Kaimal, J. M., & Andréasson, C. (2016). Luciferase NanoLuc as a reporter for gene expression and protein levels in Saccharomyces cerevisiae. *Yeast*, *33*(5), 191-200.

40. Schleif, R., Hess, W., Finkelstein, S., & Ellis, D. (1973). Induction kinetics of the L-arabinose operon of Escherichia coli. *Journal of bacteriology*, *115*(1), 9-14.

41. Mason, P. B., & Struhl, K. (2005). Distinction and relationship between elongation rate and processivity of RNA polymerase II in vivo. *Molecular cell*, *17*(6), 831-840.

42. Edwards, A. M., Kane, C. M., Young, R. A., & Kornberg, R. D. (1991). Two dissociable subunits of yeast RNA polymerase II stimulate the initiation of transcription at a promoter in vitro. *Journal of Biological Chemistry*, *266*(1), 71-75.

43. Karpinets, T. V., Greenwood, D. J., Sams, C. E., & Ammons, J. T. (2006). RNA: protein ratio of the unicellular organism as a characteristic of phosphorous and nitrogen stoichiometry and of the cellular requirement of ribosomes for protein synthesis. *BMC biology*, *4*(1), 1-10.

44. Riba, A., Di Nanni, N., Mittal, N., Arhné, E., Schmidt, A., & Zavolan, M. (2019). Protein synthesis rates and ribosome occupancies reveal determinants of translation elongation rates. *Proceedings of the national academy of sciences*, *116*(30), 15023-15032.

45. Letzring, D. P., Dean, K. M., & Grayhack, E. J. (2010). Control of translation efficiency in yeast by codon–anticodon interactions. *Rna*, *16*(12), 2516-2528.

46. Veltri, A. J., D'Orazio, K. N., Lessen, L. N., Loll-Krippleber, R., Brown, G. W., & Green, R. (2021). Distinct ribosome states trigger diverse mRNA quality control pathways. *bioRxiv*.

47. Meydan, S., & Guydosh, N. R. (2021). A cellular handbook for collided ribosomes: surveillance pathways and collision types. *Current genetics*, *67*(1), 19-26.

48. Chu, D., Kazana, E., Bellanger, N., Singh, T., Tuite, M. F., & von der Haar, T. (2014). Translation elongation can control translation initiation on eukaryotic mRNA s. *The EMBO journal*, *33*(1), 21-34.

49. Carroll, J. S., Munchel, S. E., & Weis, K. (2011). The DExD/H box ATPase Dhh1 functions in translational repression, mRNA decay, and processing body dynamics. *Journal of Cell Biology*, *194*(4), 527-537.

50. Coller, J. M., Tucker, M., Sheth, U., Valencia-Sanchez, M. A., & Parker, R. (2001). The DEAD box helicase, Dhh1p, functions in mRNA decapping and interacts with both the decapping and deadenylase complexes. *Rna*, *7*(12), 1717-1727.

51. Fischer, N., & Weis, K. (2002). The DEAD box protein Dhh1 stimulates the decapping enzyme Dcp1. *The EMBO journal*, *21*(11), 2788-2797.

52. Tseng-Rogenski, S. S. I., Chong, J. L., Thomas, C. B., Enomoto, S., Berman, J., & Chang, T. H. (2003). Functional conservation of Dhh1p, a cytoplasmic DExD/H-box protein present in large complexes. *Nucleic acids research*, *31*(17), 4995-5002.

53. Sweet, T., Kovalak, C., & Coller, J. (2012). The DEAD-box protein Dhh1 promotes decapping by slowing ribosome movement. *PLoS biology*, *10*(6), e1001342.

54. Radhakrishnan, A., Chen, Y. H., Martin, S., Alhusaini, N., Green, R., & Coller, J. (2016). The DEAD-box protein Dhh1p couples mRNA decay and translation by monitoring codon optimality. *Cell*, *167*(1), 122-132.

55. Gamble, C. E., Brule, C. E., Dean, K. M., Fields, S., & Grayhack, E. J. (2016). Adjacent codons act in concert to modulate translation efficiency in yeast. *Cell*, *166*(3), 679-690.

56. Burke, P. C., Park, H., & Subramaniam, A. R. (2021). A Nascent Peptide Code for Translational Control of mRNA Stability in Human Cells. *bioRxiv*.

57. Chan, L. Y., Mugler, C. F., Heinrich, S., Vallotton, P., & Weis, K. (2018). Non-invasive measurement of mRNA decay reveals translation initiation as the major determinant of mRNA stability. *Elife*, *7*, e32536.

58. Jungfleisch, J., Nedialkova, D. D., Dotu, I., Sloan, K. E., Martinez-Bosch, N., Brüning, L., Raineri, E., Navarro, P., Bohnsack, M. T., Leidel, S. A., & Díez, J. (2017). A novel translational control mechanism involving RNA structures within coding sequences. *Genome research*, *27*(1), 95-106.

59. Liu, X., Yao, Z., Jin, M., Namkoong, S., Yin, Z., Lee, J. H., & Klionsky, D. J. (2019). Dhh1 promotes autophagy-related protein translation during nitrogen starvation. *PLoS biology*, *17*(4), e3000219.

CHAPTER 3: Mechanisms of mRNP-directed localization of mRNAs in glucose starvation

3.1 Chapter Summary

Glucose deprivation in yeast leads to a rapid shutdown of canonical cap dependent translation initiation (Wek 2018, Simpson & Ashe 2012, Gordiyenko et al. 2019). During this time, many preexisting mRNAs are sequestered into cytoplasmic messenger ribonucleoprotein (mRNP) granules, such as P-bodies (PBs) and stress granules (SGs) (Buchan & Parker 2009, Khong et al. 2017, Teixeira et al. 2005, Jain et al. 2016, Guzikowski et al. 2019, Protter & Parker 2016). Specific classes of mRNAs are rapidly transcribed however some are translationally inhibited and sequestered into mRNP granules while others are translationally active and excluded from mRNP granules (Zid & O'Shea 2014). While transcriptomics of mRNP granules reveals correlations between transcript length, translation efficiency, and likelihood of localization to mRNP granules, the exact mechanism by which stress-induced mRNAs are either destined for translation inhibition and localization to mRNP granules or active translation and exclusion from mRNP granules remains unclear.

In this chapter, two projects that seek to discover the mechanisms underlying the relationship between translatability and mRNP localization during acute glucose starvation are discussed. In section 3.2 The Role of Rvb1/2 in Driving Cytoplasmic Granular Localization, we investigate how the SG-enriched proteins Rvb1 and Rvb2 function to direct cytoplasmic localization of newly transcribed alternative glucose metabolism genes. Our work suggests that Rvb1/2 suppresses translation of new transcripts and directs their localization into mRNP granules during glucose starvation. In section 3.3 Poor mRNA Translatability During Glucose Starvation Drives mRNP

Granule Localization, we disentangle the relationship between translatability and subcellular localization during acute glucose starvation. Preliminary work suggests that inhibition of translation increases the proportion of newly transcribed mRNAs localizing to mRNPs, indicating that poor translatability is sufficient to drive mRNP inclusion of mRNAs during stress conditions.

3.2 The Role of Rvb1/2 in Driving Cytoplasmic Granular Localization

Introduction

Cells need to rapidly adapt their transcriptomes and proteomes to changing environmental conditions to maintain cellular homeostasis. During the onset of acute stress conditions, including nutrient starvation, heat shock, and osmotic stresses, translation initiation is quickly inhibited through the phosphorylation of eIF2A, preventing the formation of a functional ternary complex (Wek 2018, Simpson & Ashe 2012, Gordiyenko et al. 2019). Concurrently during conditions of acute glucose deprivation, certain classes of stress response genes are transcriptionally induced, including heat shock genes and alternative glucose metabolism genes (Hahn & Thiele 2004, Hahn et al. 2004, Zid & O'Shea 2014, Nadal et al. 2011). However, these classes of genes differ in cytoplasmic fate: heat shock genes such as *HSP30* and *HSP26* are actively translated whereas alternative glucose metabolism genes such as *GLC3* and *HXK1* are translationally repressed. Furthermore, the subcellular localization of these stress response genes differs as well. Stress granules (SGs) and P-Bodies (PBs) are two well-known stress-induced cytoplasmic phase separated mRNP granules which are formed primarily from disordered proteins and long, non-translating mRNAs (Buchan & Parker

2009, Khong et al. 2017, Teixeira et al. 2005, Jain et al. 2016, Guzikowski et al. 2019, Protter & Parker, 2016). Transcriptomics on SG-localized mRNAs found that about 10% of bulk mRNA molecules are present in SGs and most mRNAs localize to SGs but the efficiency varies greatly (Khong et al. 2017). It has been previously shown that *HSP30* and *HSP26* mRNAs are excluded from these granules whereas GLC3 and HXK1 mRNAs are partitioned into these granules.

Previously, we have shown that promoter sequences are sufficient to drive cytoplasmic fate during glucose starvation in yeast. In specific, stress-induced mRNAs showed two different responses: mRNAs of most heat shock genes (Class I, e.g. *HSP30* and *HSP26*) were transcriptionally induced, translationally active, and were excluded from mRNPs; Class II mRNAs, enriched in alternative glucose metabolism genes (e.g. *GLC3* and *HXK1*), were transcriptionally induced, translationally inactive, and were sequestered in both SGs and PBs. As promoter sequences and translation machinery are compartmentally distinct, with promoter sequences exclusively residing in the nucleus and translation machinery in the cytoplasm, this finding suggested the existence of a promoter-specific trans-acting factor co-transcriptionally loaded onto mRNAs prior to nuclear export that functioned to direct translatability and cytoplasmic localization.

Proteomic analysis of SGs found that both yeast and mammalian SGs were enriched for Rvb1 and Rvb2 (RuvbL1 and RuvbL2 in mammals, respectively), two highly conserved AAA+ (ATPases Associated with various cellular Activities) proteins with functions in chromatin remodeling and other nuclear pathways (Jain et al. 2016, Huen et al. 2010, Jha & Dutta 2009, Nano & Houry 2013, Tian et al. 2017). Structural

studies of the Rvb complex have shown that it forms a dodecamer composed of a hexameric Rvb1 ring stack on a hexameric Rvb2 ring. Furthermore, Rvb1/2 have been shown to regulate the dynamics and size of SGs (Narayanan et al. 2019, Zaarur et al. 2015). Using a novel proteomics-based screening method to identify co-transcriptionally loaded protein factors, we found that Rvb1 and Rvb2 were enriched on transcripts from Class II promoters as compared to transcripts from Class I promoters. Additionally, using both chromatin immunoprecipitation (ChIP) and RNA immunoprecipitation (RIP), we found Rvb1/2 to be enriched on Class II promoters and Class II-promoted mRNAs during glucose starvation. Rvb1/2's DNA interactions, RNA interactions, and their role in SG dynamics suggests the potential of Rvb1/2 as a factor that may contribute to promoter-specified cytoplasmic fate. In this section, we explore the effect of Rvb1/2 in directing subcellular localization of newly transcribed mRNAs during glucose starvation. We find that artificially tethering Rvb1 or Rvb2 to a Class I promoter-driven mRNA significantly increases its granule localization during glucose starvation.

Results

To investigate how Rvb1 and Rvb2 can affect subcellular localization of mRNAs, we created a construct with a *HSP30* promoter (Class I), nanoluciferase ORF, a PP7 stem loop, and MS2 stem loops (Figure 3.2.1). The *HSP30* promoter has been shown to be sufficient to drive stress-induced transcription, active translation, and exclusion from mRNA granules during glucose starvation (Zid & O'Shea 2014). This construct was transformed into a yeast strain expressing Rvb1 C-terminally fused to PP7 coat protein (PCP; Rvb1-PCP), Rvb2 C-terminally fused to PCP (Rvb2-PCP), or neither protein

containing a PCP (PP7 ctrl). The PCP fused to either Rvb1 or Rvb2 would bind to the PP7 stem loop found in the transcript. Additionally, each yeast strain expressed GFP-MCP and Dcp2-RFP to fluorescently label mRNA and PBs, respectively. As Rvb1 and Rvb2 did not display strong binding to the promoters and mRNAs of Class I genes (e.g. *HSP30*), we specifically tethered Rvb1 and Rvb2 to a Class I promoter-driven mRNA to see how it would affect localization.

We found that tethering Rvb1/Rvb2 significantly increases the granular localization of our construct as compared to the PP7 control strain in glucose starvation. Only 4% of cells in the PP7 control strain contained *HSP30* promoter-driven mRNA-containing granules whereas the percentage increased to 27% for Rvb1-tethered mRNA and 39% for Rvb2-tethered mRNA (Figures 3.2.2 and 3.2.3). Furthermore, most of the mRNA-containing granules do not colocalize with PBs, suggesting that these foci are distinct from PBs.

Discussion

Here, our results demonstrate a novel function of the AAA+ ATPases Rvb1 and Rvb2 in cytoplasmic localization of transcripts into mRNP granules. We showed that tethering Rvb1 or Rvb2 to a *HSP30*-promoted mRNA, which normally exhibits active translation and exclusion from mRNP granules, was sufficient to significantly increase the localization of mRNAs to mRNP granules during glucose starvation. Other work described in the paper showed that tethering Rvb1 or Rvb2 to mRNAs significantly increased transcription but decreased translation of bound mRNAs. These functions of transcription induction, translation inhibition, and mRNP-localization are characteristics

of the behavior of observed in Class II promoted-genes during glucose starvation and may explain how Class I genes are differentiated from Class II genes. Furthermore, this finding, combined with other findings discussed in the paper on the enrichment of Rvb1/2 on promoters of Class II alternative glucose metabolism genes and mRNA, suggests Rvb1/2's role in coupling transcription, translation, and localization of Class II genes during glucose starvation.

Taken together, we hypothesize a model where Rvb1/2 are co-transcriptionally loaded onto Class II-promoted mRNAs prior to nuclear export and upon reaching the cytoplasm, inactivates translation and directs localization to mRNP granules. The coupling of transcription and cytoplasmic fate may be an adaptive mechanism for cells to both mitigate stress and prepare for the post-stress recovery. For example, allowing active translation of stress response factors to mitigate immediate cellular stresses while preventing translation of genes which may play a role in stress recovery once the stressor has abated. We find that Rvb1/2 are enriched at promoters of alternative glucose metabolism genes during glucose starvation but it would be interesting to see if Rvb1/2 are recruited to other types of genes upon different stressors, such as heat shock and oxidative stress. Additionally, further experiments must be done to determine how Rvb1/2 are recruited to Class II promoters and how it functions to inhibit translation and direct mRNP granule localization during stress conditions.

Materials and Methods

Yeast Strains and Plasmids. All yeast strains, plasmids, and oligonucleotides used in this study are listed in Table 3.2.1, Table 3.2.2, and Table 3.2.3, respectively.

The yeast background strain W303 (EY0690) was used for all experiments. Transformed yeast strains were created through genomic integration of a linearized plasmid using homologous recombination. In yeast cloning for the C-terminal fusion on endogenous proteins (e.g. Rvb1-PCP, Rvb2-PCP), we used plasmids of the Pringle pFA6a and pKT systems, gifts from the E. K. O'Shea laboratory and the K. Thorn laboratory. We modified the pFA6a and pKT plasmids by inserting in peptides of interest into the plasmids. The primers used to amplify the fragments from these plasmids contain 2 parts from 3' to 5': a uniform homolog sequence to amplify the plasmid and a homolog sequence to direct insertion of the fragments to the genomic loci of interest. The fragments were transformed into yeast and integrated into the genome via homologous recombination. The integrations were confirmed by genomic DNA PCR (Yeast DNA Extraction Kit from Thermo Fisher). In the cloning of the reporter strains, we used a strain that was derived from W303 and has one copy of a genomic insertion of MYOpr-MS2CP-2xGFP and an endogenous fusion protein Dcp2-mRFP, as the background strain. Further, we transformed the linearized MS2-loop-containing reporter plasmids into the strain by restriction digestion and genomic integration. To generate the MS2-loop-containing reporter plasmids, we started from the plasmid ZP15 pRS305-12XMS2-tAdh1. ZP15 was linearized by the restriction enzymes SacII and NotI (New England Biosciences). Promoter fragments, nanoluciferase-PEST CDS fragments were inserted into linearized ZP15 using Gibson Assembly. Promoter sequences were amplified by PCR from W303 genomic DNA. Nanoluciferase-PEST CDS was amplified by PCR from a geneblock. To generate the PP7-MS2-containing reporter plasmids (ZP296 pRS305-HSP30prUTR-nLuc-PEST-1xPP7-12xMS2-tAdh1), ZO680 and ZO679

were first annealed using the primer annealing protocol described by Thermo Fisher. ZP15 was linearized by restriction digest using BamHI and NotI (New England Biosciences). Promoter fragments, nanoluciferase-PEST CDS fragments were inserted into linearized ZP440 using Gibson assembly.

Yeast Growth and Media. For cells cultured in functional experiments, cells were streaked out on yeast extract peptone dextrose (YPD) agarose plates (BD Biosciences) from frozen stocks and grew at 30°C for 2 days. Single colonies were selected to start overnight cultures for each biological replicate. Cells were grown at 30°C in a spinning rotor in synthetic complete glucose media (SCD media: yeast nitrogen base from RPI, glucose from Sigma-Aldrich, Hopkin's Synthetic Complete Amino Acid Mixture from Sunrise Sciences). When the OD660 of cells reached 0.4, half of the culture was harvested as the pre-starved sample. The remaining half of the culture was transferred to prewarmed synthetic complete media lacking glucose (SC -G media) by centrifugation. Cells were centrifuged at 3000 *x g*, washed once using SC -G media, and resuspended in SC -G media to an equivalent volume as the pre-starved sample in SCD media. Glucose starvation was performed in a spinning rotor at 30°C. The duration of glucose starvation varied from 15 to 30 minutes depending on experiment.

Live-Cell Microscopy and Analysis. Cells were grown to an OD660 to ~0.4 in SCD medium at 30°C and glucose-starved in SC -G medium for 15 and 30 minutes. 100 µL of cell culture was loaded onto a 96-well glass-bottom microplate (Cellvis). Cells were imaged using an Eclipse Ti-E microscope (Nikon) with an oil-immersion 63x

objective. Imaging was controlled using NIS-Elements software (Nikon). Imaging analysis was performed on Fiji software.

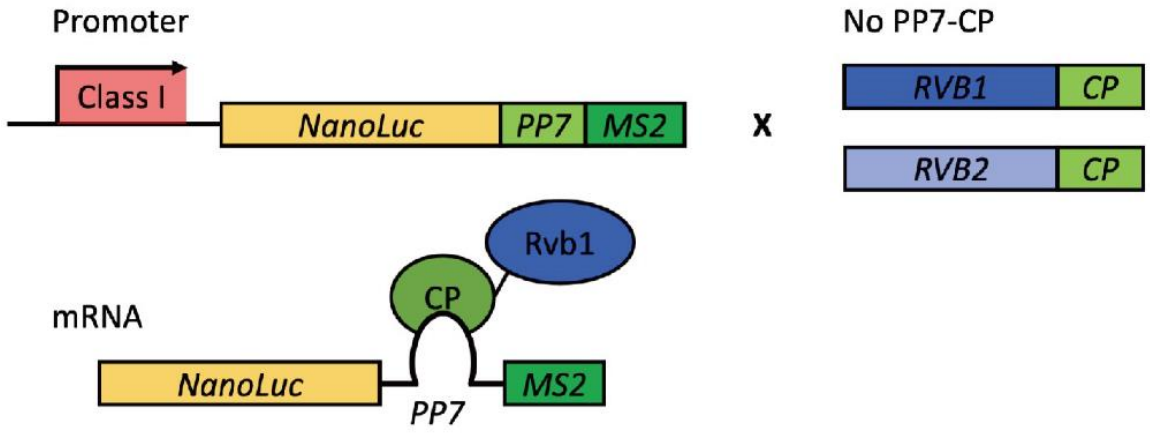

Figure 3.2.1 Schematic of Rvb1/2 constructs. Construct consists of a *HSP30* promoter (Class I), nanoluciferase CDS, PP7 stem loop, and 12 tandem MS2 stem loops. Rvb1 or Rvb2 are C-terminally fused with PP7 coat protein (CP). Upper panel shows plasmid construct and co-expressed fusion Rvb proteins. Lower panel shows tethering of Rvb1-CP fusion to the transcribed mRNA.

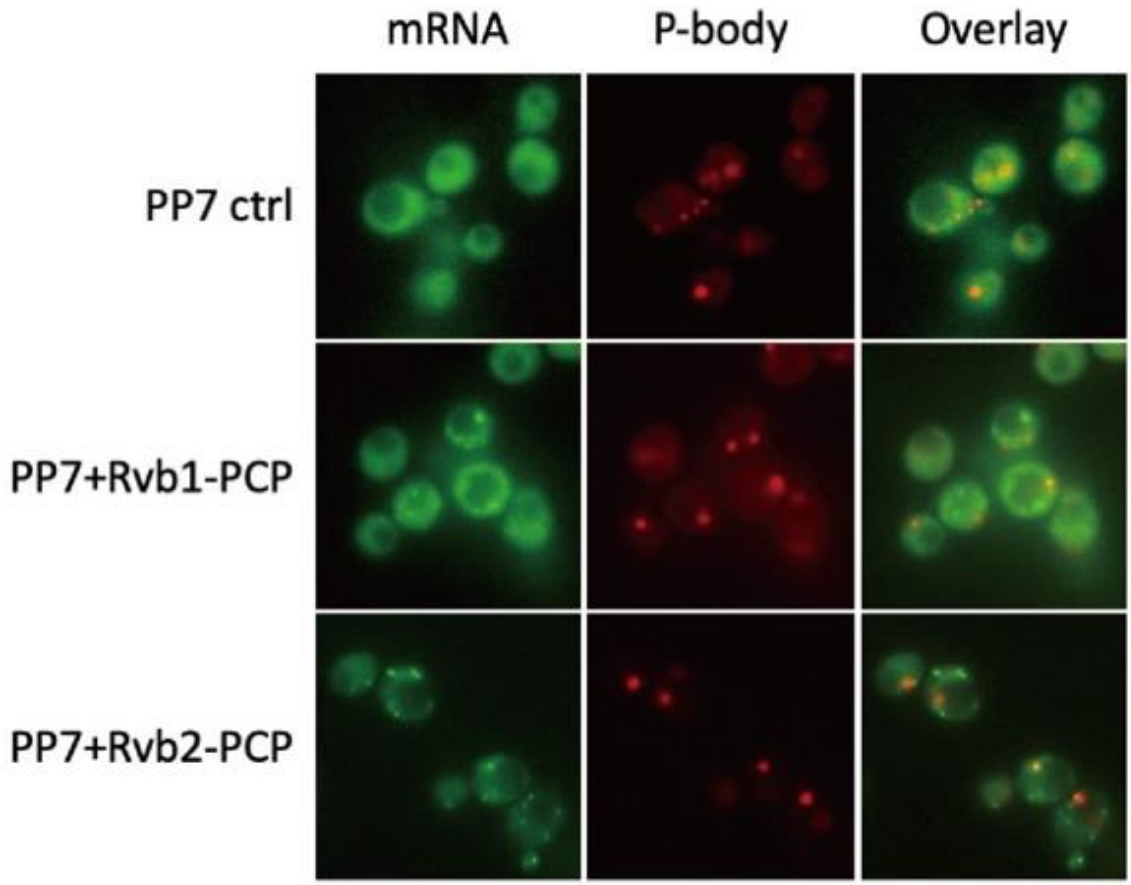

Figure 3.2.2 Live imaging of 30-minute glucose starved yeast. Live images of yeast showing the subcellular localization of the *HSP30*-promoter driven mRNA after 30 minutes of glucose starvation. Reporter mRNAs are labeled using expressed MCP-GFP binding to MS2 stem loops in the mRNA. P-bodies are labeled by the p-body marker Dcp2 fused to mCherry. PP7 Ctrl: negative control, neither Rvb1 or Rvb2 is used to PP7 coat protein (PCP). PP7+Rvb1-PCP: Rvb1 is tethered to construct mRNA. PP7-Rvb2-PCP: Rvb2 is tethered to construct mRNA.

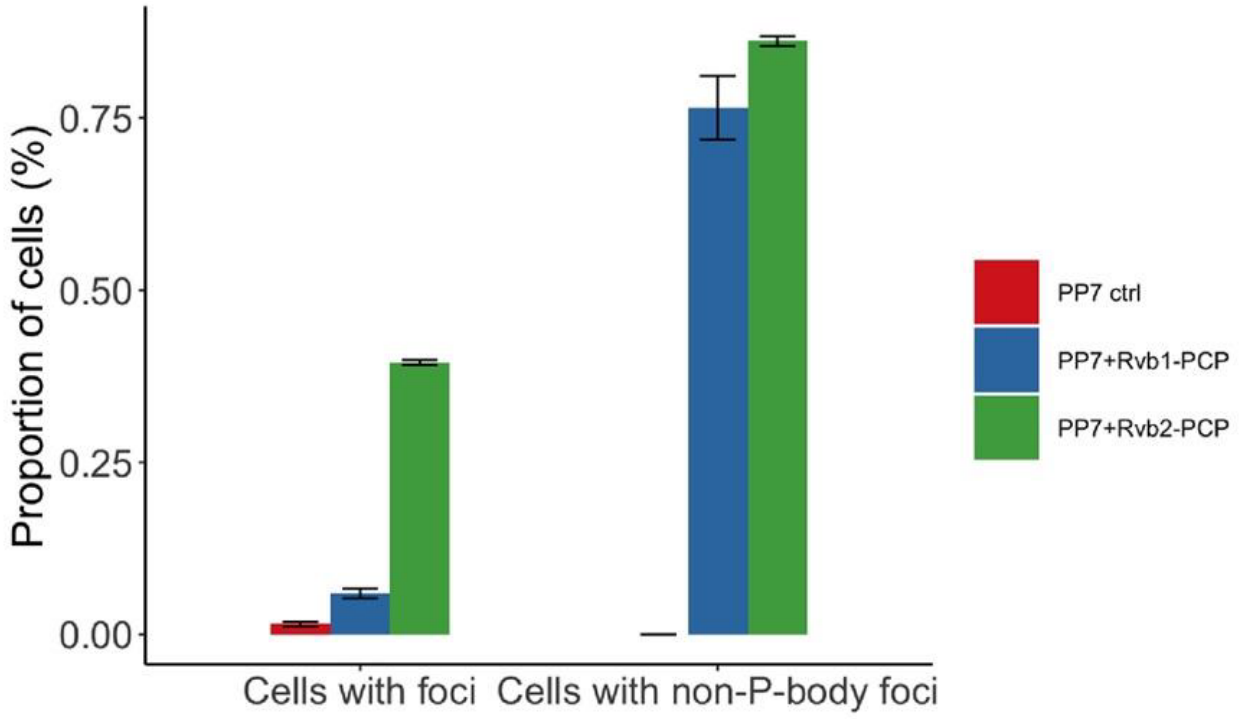

Figure 3.2.3 Quantification of foci after 30-minute glucose starvation.
Quantification of reporter mRNA-containing granules and p-bodies after 30 minutes of glucose starvation. Cells with foci: percentage of cells that contain at least one mRNA-containing granule. Cells with non-P-body foci: Percentage of cells that contain at least one mRNA-containing granule and have no colocalization with P-bodies. N=200. Error bars are from 2 biological replicates.

Table 3.2.1 List of yeast strains used in Rvb study

Identifier	Genotype
W303	(EY0690) MATa trp1 leu2 ura3 his3 can1 GAL+ psi+
ZY18	W303; MYO2pr-MCP-2xGFP; Dcp2-RFP
ZY266	ZY18; HSP30prUTR-nLucPEST-1xPP7-12xMS2-tADH1
ZY314	ZY18; Rvb1-PCP-6xHis; HSP30prUTR-nLucPEST-1xPP7-12xMS2-tADH1
ZY315	ZY18; Rvb2-PCP-6xHis; HSP30prUTR-nLucPEST-1xPP7-12xMS2-tADH1
ZY316	ZY18; Rvb1-PCP-6xHis
ZY317	ZY18; Rvb2-PCP-6xHis

Table 3.2.2 List of plasmids used in Rvb study

Identifier	Construct
ZP15	pRS305-12xMS2-tADH1
ZP296	pRS305-HSP30prUTR-nLucPEST-1xPP7-12xMS2-tADH1
ZP311	pKT-PCP-6xHis-tADH1
ZP440	pRS305-1xPP7-12xMS2-tADH1

Table 3.2.3 List of primers used in Rvb study

Identifier	Description	Sequence
ZO463	Amplifies nLucPEST (F)	ATGGTTTTTACTTTAGAAGATTTTG
ZO464	Amplifies nLucPEST with homology to reporter vector (R)	ATCCACTAGTTCTAGAGCTTAAACATTAATACGAGCAGAAG
ZO470	Amplifies HSP30prUTR with homology to reporter vector (R)	TCTAAAGTAAAAACCATTTGAAATTTGTTGTTTTTAGTAATCAA
ZO679	PP7 stem loop with NotI/BamHI overhangs (F)	GGCCGCTTAAGGAGTTTATATGGAAACCCTTAG
ZO680	PP7 stem loop with NotI/BamHI overhangs (R)	GATCCTAAGGGTTTCCATATAAACTCCTTAAGC
ZO802	Rvb1 C-terminal tagging of pKT vector	AAGGTCAACAAAGATTTTAGAAACTTCCGCAAATTATTTGGGTGACGGTGCTGGTTTA
ZO803	Rvb1 C-terminal tagging of pKT vector	TATTTTTATTTATGAAATGTGCTTTAGGCTTTCTTCACTGTCGATGAATTCGAGCTCG
ZO804	Rvb2 C-terminal tagging of pKT vector	TGCTAAATCAGCAGACCCTGATGCCATGGATACTACGGAAGGTGACGGTGCTGGTTTA
ZO805	Rvb2 C-terminal tagging of pKT vector	TATATATTTGATGCAATTTCTGCCTTAAAGTACAAAATGCTCGATGAATTCGAGCTCG
ZO966	Amplifies HSP30prUTR with homology to reporter vector (F)	TCACTATAGGGCGAATTGGAGCTCCACCGCCCTTTCTTCAAAAGTAGAAAACTTG

3.3 Poor mRNA Translatability During Glucose Starvation Drives mRNP Granule Localization

Introduction

Processing bodies (PBs) and stress granules (SGs) are cytoplasmic, phase-separated messenger ribonucleoprotein (mRNP) granules that form during stress conditions in eukaryotic cells. These mRNP granules are enriched in proteins containing intrinsically disordered regions (IDRs) and long, non-translating mRNAs (Jain et al. 2016, Khong et al. 2017, Guzikowski et al. 2019, Buchan & Parker 2009). Transcriptomics on SGs has shown that up to 10% of the bulk mRNA in the cell are sequestered into these granules; most mRNA species are represented however the efficiency to which they are sequestered varies greatly. It has been previously shown that certain mRNAs, especially those undergoing active translation during stress conditions such as stress response genes, are excluded from mRNP granules and remain diffuse in the cytoplasm (Khong et al. 2017, Zid & O'Shea 2014).

There is a strong correlation between translatability and mRNP localization: translationally active mRNAs are excluded from mRNP granules whereas translationally inactive mRNAs are sequestered into mRNP granules. Indeed, a current model of mRNA integration into SGs theorizes that ribosomes prevent mRNAs from condensing into aggregates by limiting exposed coding regions that can form RNA-RNA interactions which are crucial for SG formation (Van Treeck et al. 2018, Moon et al. 2019, Lee & Seydoux 2019). As canonical translation initiation is inhibited upon the onset of stress, ribosomes will run off most transcripts, shifting them to an inactive translation state, leaving them devoid of ribosomes, and exposing them to RNA-RNA interactions. While

this model suggests that mRNP granule localization is a consequence of poor translatability, direct evidence of this relationship has been lacking.

Previously, our lab has shown that promoter sequences were sufficient to control both translatability and subcellular localization during glucose starvation (Zid & O'Shea 2014). In particular, HSP30's promoter has been shown to drive active transcription, translation, and exclusion of mRNAs from mRNP granules. We reasoned that if active translation was necessary for exclusion from mRNP granules, inhibition of translation would lead to sequestration to mRNP granules. In this section, we explore the relationship between translatability and mRNP granule localization during glucose starvation through translation inhibition of a normally well-translated and mRNP granule-excluded mRNA. Preliminary data suggests that inhibiting translation through the addition of a GC-rich stem loop at the translation start site significantly increases mRNP granule localization of our HSP30 promoter-driven mRNA construct.

Results

We created a construct in which we inserted the endogenous yeast HSP30 promoter and 5'UTR upstream of a cyan fluorescent protein (CFP) open reading frame (ORF) (Figure 3.3.1). We attached 12 tandem MS2 stem loops to the 3' end of our construct for mRNA visualization through expression of a MS2 Coat Protein (MCP) and green fluorescent protein (GFP) fusion protein. To inhibit translation, we inserted a SfiI restriction site upstream of the CFP or nLuc ORFs (between positions -7 and -6); a construct that lacked this SfiI restriction site was used as a control. Addition of an SfiI restriction site proximal to the AUG start codon has been shown to strongly inhibit

protein expression levels of its corresponding downstream gene in yeast (Lamping et al. 2013).

As an initial assessment, we tested protein expression of a nLuc-containing construct to confirm if protein expression was inhibited. We found that addition of a proximal SfiI restriction site strongly inhibited protein expression of our nLuc-containing construct after 20 minutes of glucose starvation, down to approximately 1% of the control expression (data not shown). As we confirmed that protein expression was inhibited, we then assessed how mRNP granule localization was affected. We imaged yeast cells after 20 minutes of glucose starvation and quantified the number of cells that contained granules enriched in our CFP-containing mRNA (Figure 3.3.2). Addition of the SfiI restriction site significantly increased the percentage of cells expressing construct mRNA-containing granules (Figure 3.3.3).

Discussion

Current models of mRNA localization during acute stress conditions point to ribosome runoff as a prerequisite to mRNP localization. Our preliminary data shows that in constructs where translation is strongly inhibited, localization of construct mRNA to mRNP granules significantly increased, consistent with current models. A more nuanced look at mechanisms of mRNA localization during stress suggests that active translation may not be necessary for mRNP exclusion but instead ribosome loading on mRNAs to prevent RNA-RNA interactions may be the driving factor. Indeed, it has been shown that addition of the drug cycloheximide, a translation elongation inhibitor, abolishes and prevents formation of SGs (Mollet et al. 2008, Kedersha et al. 2005,

Aulas et al. 2017). In arresting elongating ribosomes on mRNAs, mRNAs are unable to create RNA-RNA interactions to nucleate SGs. Under normal stress conditions, mRNAs undergoing continual translation initiation and elongation will be excluded from SGs while other mRNAs will eventually become devoid of ribosomes and sequester into SGs. Further work is necessary to characterize the factors that determine if an mRNA will be actively translated or be translationally inhibited.

Materials and Methods

Yeast Strains and Plasmids. All yeast strains, plasmids, and oligonucleotides used in this study are listed in Table 3.3.1, Table 3.3.2, and Table 3.3.3, respectively. The yeast background strain W303 (EY0690) was used for all experiments. Transformed yeast strains were created through genomic integration of a linearized plasmid using homologous recombination. In the cloning of the reporter strains, we used a strain that was derived from W303 and has one copy of a genomic insertion of MYOpr-MS2CP-2xGFP and an endogenous fusion protein Dcp2-mRFP, as the background strain (ZY18). To generate the reporter plasmids, we started from the plasmids ZP27 pRS305-HSP30prUTR-CFP-12xMS2(v4) and ZP207 pRS305-HSP30prUTR-nLucPEST-12xMS2(v4). We used PCR and primers targeting the beginning of either the CFP or nLucPEST CDS as the forward primer and a primer targeting HSP30 5'UTR as the reverse primer to linearize the plasmid. SfiI restriction sites (CCGGCGAGCCCGG) were incorporated into PCR primers as an overhang and joined together via using Hi-Fi DNA Assembly Master Mix (New England Biosciences).

Yeast Media and Growth. For cells cultured in functional experiments, cells were streaked out on yeast extract peptone dextrose (YPD) agarose plates (BD Biosciences) from frozen stocks and grew at 30°C for 2 days. Single colonies were selected to start overnight cultures for each biological replicate. Cells were grown at 30°C in a spinning rotor in synthetic complete glucose media (SCD media: yeast nitrogen base from RPI, glucose from Sigma-Aldrich, Hopkin's Synthetic Complete Amino Acid Mixture from Sunrise Sciences).

Nanoluciferase Protein Expression Assay. Yeast cultures were grown overnight at 30°C in a spinning rotor. When the OD600 of cells reached 0.5, the culture was transferred to prewarmed synthetic complete media lacking glucose (SC -G media) by centrifugation. Cells were centrifuged at 3000 *x g*, washed once using SC -G media, and resuspended in SC -G media to the same volume taken for glucose starvation. Tubes were placed back into a spinning rotor at 30°C for 15 minutes. 90 µL of each culture was placed in separate wells in a 96-well white flat bottom plate (Grainger) and to each well, 10 µL of Nano-Glo Luciferase Substrate (Promega; 1:100 Nano-Glo Luciferase Substrate in Nano-Glo Luciferase Assay Buffer) was added. The plate was loaded onto a Tecan Infinite 200Pro prewarmed to 30°C and the following Tecan i-control script was used: (1) Kinetic Cycle: [Cycle Duration: 5 minutes, Kinetic Interval: 30 seconds], (2) Shaking: [Duration: 3 seconds, Mode: Orbital, Amplitude 2 mm], (3) Luminescence: [Attenuation: Automatic, Integration Time: 1000 ms, Settle Time: 0 ms]. Protein expression at the 5-minute timepoint was used for normalization.

Live-Cell Microscopy and Analysis. Yeast cultures were grown overnight to an OD600 of ~0.2 in SCD medium at 30°C and glucose-starved in SC -G medium for 20

minutes. 100 µL of cell culture was loaded onto a 96-well glass-bottom microplate (Cellvis). Cells were imaged using an Eclipse Ti-E microscope (Nikon) with an oil-immersion 63x objective. Imaging was controlled using NIS-Elements software (Nikon). Imaging analysis was performed on Fiji software.

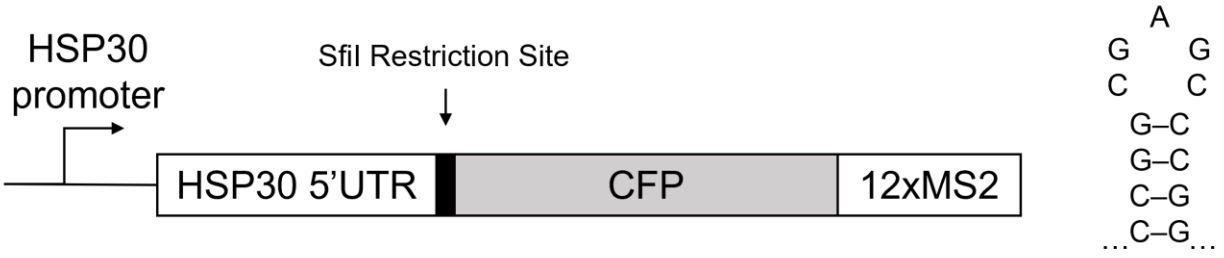

Figure 3.3.1 Schematic of SfiI reporter construct. Left panel: Schematic of SfiI reporter constructs containing yeast endogenous *HSP30* promoter and 5'UTR, SfiI restriction site, CFP open reading frame, and 12 tandem MS2 stem loops. The SfiI restriction site is placed proximal to the AUG translation start site at between positions -7 and -6. MS2 stem loops are recognized and bound by expressed MS2 coat protein fused to GFP for subcellular visualization of mRNA localization. Right panel: representation of the SfiI restriction site that forms a GC-rich stem loop.

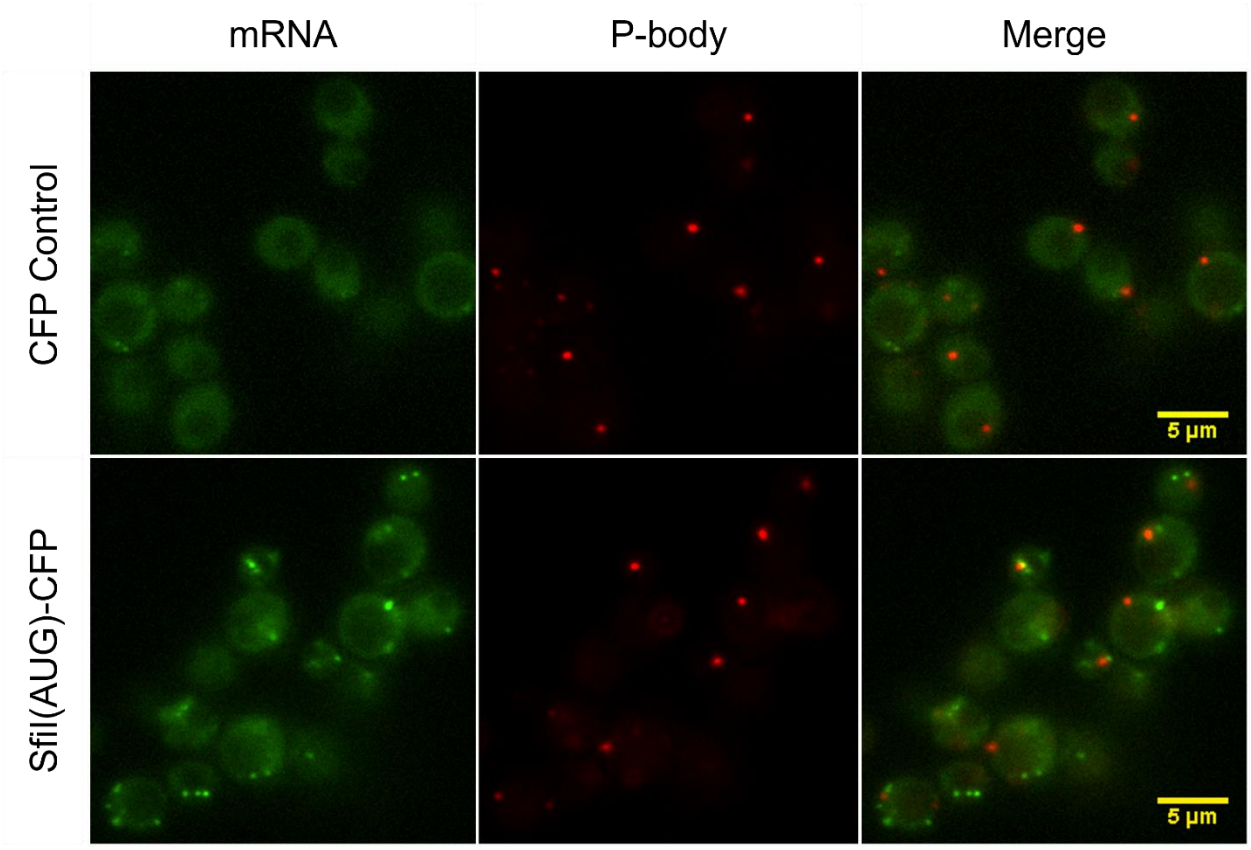

Figure 3.3.2 Live imaging of 20-minute glucose starved yeast. Live images of yeast showing the subcellular localization of the SfiI-containing constructs after 20 minutes of glucose starvation. Reporter mRNAs are labeled using expressed MCP-GFP binding to MS2 stem loops in the mRNA. P-bodies are labeled by the p-body marker Dcp2 fused to mCherry. CFP Control: *HSP30*-promoter driven construct lacking SfiI stem loops. SfiI(AUG)-CFP: *HSP30*-promoter driven construct containing a SfiI stem loop proximal to the AUG start codon. Scale bar represents 5 microns.

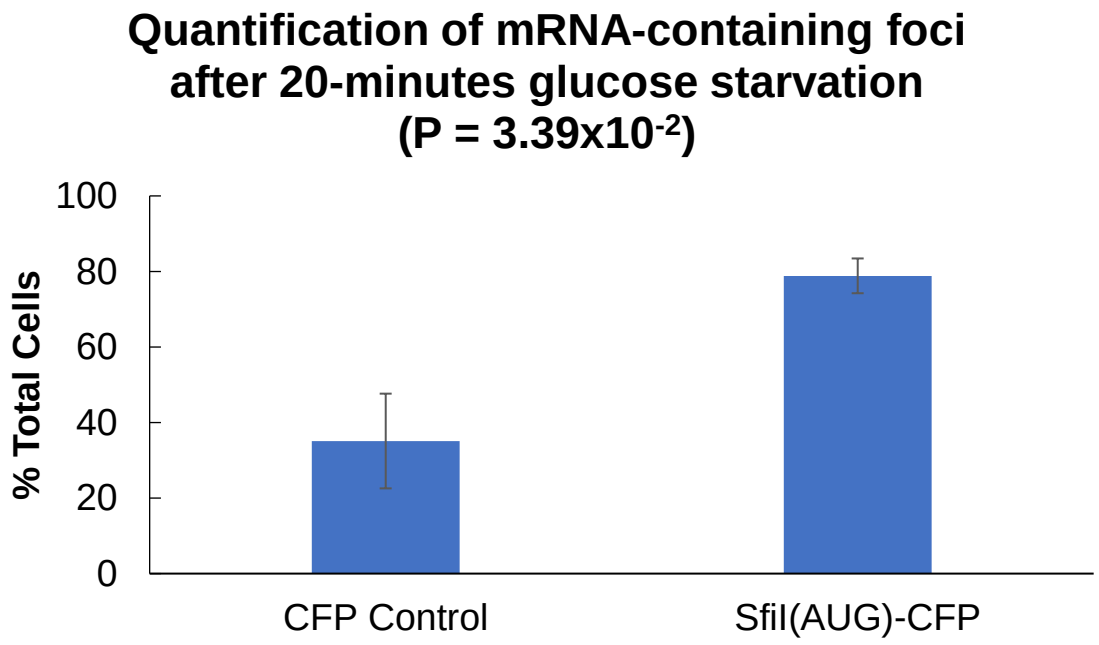

Figure 3.3.3 Quantification of foci after 20-minute glucose starvation. Comparison of reporter mRNA-containing foci after 20 minutes of glucose starvation. Each stressed cell was quantified based on if it contained at least one reporter mRNA-containing foci. CFP Control: reporter construct lacking a SfiI restriction site. N=587 from 3 biological replicates. SfiI(AUG)-CFP: reporter construct containing a SfiI restriction site proximal to the AUG translation start site. N=532 from 6 biological replicates. Error bars represent standard deviation.

Table 3.3.1 List of yeast strains used in SfiI study

Identifier	Genotype
W303	(EY0690) MATa trp1 leu2 ura3 his3 can1 GAL+ psi+
ZY18	W303; MYO2pr-MCP-2xGFP; Dcp2-RFP
ZY26	ZY18; HSP30prUTR-CFP-12xMS2(v4)
ZY193	ZY18; HSP30prUTR-nLucPEST-12xMS2(v4)
ZY330	ZY18; SfiI(AUG)_HSP30prUTR-CFP-12xMS2(v4)
ZY332	ZY18; SfiI(AUG)_HSP30prUTR-nLucPEST-12xMS2(v4)

Table 3.3.2 List of plasmids used in SfiI study

Identifier	Construct
ZP15	pRS305-12xMS2(v4)
ZP27	pRS305-HSP30prUTR-CFP-12xMS2(v4)
ZP207	pRS305-HSP30prUTR-nLucPEST-12xMS2(v4)
ZP336	SfiI(AUG)_HSP30prUTR-CFP-12xMS2
ZP338	SfiI(AUG)_HSP30prUTR-nLucPEST-12xMS2

Table 3.3.3 List of primers used in SfiI study

Identifier	Description	Sequence
ZO663	Amplifies HSP30 5'UTR and adds SfiI overhang (R)	GGCCCGAGCGGCCTTTGTTGTTTTTAGTAATCAAAAGATATTAAAG
ZO664	Amplifies CFP and adds SfiI overhang (F)	AAAGGCCGCTCGGGCCTTTCAAATGTCTAAGGGTGAAGAATT
ZO812	Sequencing primer: downstream of HSP30 promoter (F)	GAGAGTCTTCAATTATTTAGCG
ZO813	Sequencing primer: upstream of CFP (R)	GTGACCGTTAACGTCACC
ZO814	Sequencing primer: upstream of nLuc (R)	GATCTAAATTATAACCAGCAG
ZO815	Amplifies nLuc and adds SfiI overhang (F)	AAAGGCCGCTCGGGCCTTTCAAATGGTTTTTACTTTAGAAG

3.4 Acknowledgments

Chapter 3 consists of both published and unpublished material. Section 3.2, in part, is a partial reprint of the following published manuscript: Chen, YS, Tracy, S, Harjono, V, Xu, F, Moresco, JJ, Yates, JR, and Zid, BM. Rvb1/Rvb2 proteins couple transcription and translation during glucose starvation. *bioRxiv* (2021). https://doi.org/10.1101/2021.10.17.464753. The dissertation author is the third author of this paper. Section 3.3 consists of unpublished material. The dissertation author is the primary author of this material.

3.5 References

1. Wek, R. C. (2018). Role of eIF2α kinases in translational control and adaptation to cellular stress. *Cold Spring Harbor Perspectives in Biology*, *10*(7), a032870.

2. Simpson, C. E., & Ashe, M. P. (2012). Adaptation to stress in yeast: to translate or not?. *Biochemical Society Transactions*, *40*(4), 794-799.

3. Gordiyenko, Y., Llácer, J. L., & Ramakrishnan, V. (2019). Structural basis for the inhibition of translation through eIF2α phosphorylation. *Nature communications*, *10*(1), 1-11.

4. Buchan, J. R., & Parker, R. (2009). Eukaryotic stress granules: the ins and outs of translation. *Molecular cell*, *36*(6), 932-941.

5. Khong, A., Matheny, T., Jain, S., Mitchell, S. F., Wheeler, J. R., & Parker, R. (2017). The stress granule transcriptome reveals principles of mRNA accumulation in stress granules. *Molecular cell*, *68*(4), 808-820.

6. Teixeira, D., Sheth, U., Valencia-Sanchez, M. A., Brengues, M., & Parker, R. (2005). Processing bodies require RNA for assembly and contain nontranslating mRNAs. *Rna*, *11*(4), 371-382.

7. Jain, S., Wheeler, J. R., Walters, R. W., Agrawal, A., Barsic, A., & Parker, R. (2016). ATPase-modulated stress granules contain a diverse proteome and substructure. *Cell*, *164*(3), 487-498.

8. Guzikowski, A. R., Chen, Y. S., & Zid, B. M. (2019). Stress-induced mRNP granules: form and function of processing bodies and stress granules. *Wiley Interdisciplinary Reviews: RNA*, *10*(3), e1524.

9. Protter, D. S., & Parker, R. (2016). Principles and properties of stress granules. *Trends in cell biology*, *26*(9), 668-679.

10. Zid, B. M., & O'Shea, E. K. (2014). Promoter sequences direct cytoplasmic localization and translation of mRNAs during starvation in yeast. *Nature*, *514*(7520), 117-121.

11. Hahn, J. S., & Thiele, D. J. (2004). Activation of the Saccharomyces cerevisiae heat shock transcription factor under glucose starvation conditions by Snf1 protein kinase. *Journal of Biological Chemistry*, *279*(7), 5169-5176.

12. Hahn, J. S., Hu, Z., Thiele, D. J., & Iyer, V. R. (2004). Genome-wide analysis of the biology of stress responses through heat shock transcription factor. *Molecular and cellular biology*, *24*(12), 5249-5256.

13. De Nadal, E., Ammerer, G., & Posas, F. (2011). Controlling gene expression in response to stress. *Nature Reviews Genetics*, *12*(12), 833-845.

14. Huen, J., Kakihara, Y., Ugwu, F., Cheung, K. L., Ortega, J., & Houry, W. A. (2010). Rvb1–Rvb2: Essential ATP-dependent helicases for critical complexes. *Biochemistry and Cell Biology*, *88*(1), 29-40.

15. Jha, S., & Dutta, A. (2009). RVB1/RVB2: running rings around molecular biology. *Molecular cell*, *34*(5), 521-533.

16. Nano, N., & Houry, W. A. (2013). Chaperone-like activity of the AAA+ proteins Rvb1 and Rvb2 in the assembly of various complexes. *Philosophical Transactions of the Royal Society B: Biological Sciences*, *368*(1617), 20110399.

17. Tian, S., Yu, G., He, H., Zhao, Y., Liu, P., Marshall, A. G., Demeler, B., Stagg, S. M., & Li, H. (2017). Pih1p-Tah1p puts a lid on hexameric AAA+ ATPases Rvb1/2p. *Structure*, *25*(10), 1519-1529.

18. Narayanan, A., Meriin, A., Andrews, J. O., Spille, J. H., Sherman, M. Y., & Cisse, I. I. (2019). A first order phase transition mechanism underlies protein aggregation in mammalian cells. *Elife*, *8*, e39695.

19. Zaarur, N., Xu, X., Lestienne, P., Meriin, A. B., McComb, M., Costello, C. E., Newnam, G. P., Ganti, R., Romanova, N. V., Shanmugasundaram, M., Silva, S. T., Bandeiras, T. M., Matias, P. M., Lobachev, K. S., Lednev, I. K., Chernoff, Y. O., & Sherman, M. Y. (2015). RuvbL1 and RuvbL2 enhance aggresome formation and disaggregate amyloid fibrils. *The EMBO journal*, *34*(18), 2363-2382.

20. Van Treeck, B., Protter, D. S., Matheny, T., Khong, A., Link, C. D., & Parker, R. (2018). RNA self-assembly contributes to stress granule formation and defining the stress granule transcriptome. *Proceedings of the National Academy of Sciences*, *115*(11), 2734-2739.

21. Moon, S. L., Morisaki, T., Khong, A., Lyon, K., Parker, R., & Stasevich, T. J. (2019). Multicolour single-molecule tracking of mRNA interactions with RNP granules. *Nature cell biology*, *21*(2), 162-168.

22. Lee, C. Y., & Seydoux, G. (2019). Dynamics of mRNA entry into stress granules. *Nature cell biology*, *21*(2), 116-117.

23. Lamping, E., Niimi, M., & Cannon, R. D. (2013). Small, synthetic, GC-rich mRNA stem-loop modules 5′ proximal to the AUG start-codon predictably tune gene expression in yeast. *Microbial cell factories*, *12*(1), 1-19.

24. Mollet, S., Cougot, N., Wilczynska, A., Dautry, F., Kress, M., Bertrand, E., & Weil, D. (2008). Translationally repressed mRNA transiently cycles through stress granules during stress. *Molecular biology of the cell*, *19*(10), 4469-4479.

25. Kedersha, N., Stoecklin, G., Ayodele, M., Yacono, P., Lykke-Andersen, J., Fritzler, M. J., Scheuner, D., Kaufman, R. J., Golan, D. E., & Anderson, P. (2005). Stress granules and processing bodies are dynamically linked sites of mRNP remodeling. *Journal of Cell Biology*, *169*(6), 871-884.

26. Aulas, A., Fay, M. M., Szaflarski, W., Kedersha, N., Anderson, P., & Ivanov, P. (2017). Methods to classify cytoplasmic foci as mammalian stress granules. *Journal of visualized experiments: JoVE*, (123).

CHAPTER 4: Future Directions and Concluding Remarks

4.1 Future Directions

The development of an *in vivo* eukaryotic elongation reporter is an important next step in unraveling the complexities in protein translation regulation. While we have demonstrated its use in studying codons and elongation stalls in their relation to rescue pathways and effects on gene expression, much work remains in both the improvement of our assay and the potential this tool represents. One major improvement area is to reduce the variability of the protein expression patterns across replicates as protein expression is tied directly to calculations of elongation rate. While we find that protein expression normalized to an internal control within biological replicates is relatively consistent, there is a great deal of variability when comparing between replicates despite normalizing for the density of cultures as measured by OD600. It remains unclear whether this is due to subtle differences in growth conditions and handling of each scientist or other factors including age of the yeast, consistency in growth media, or experimental setup. Furthermore, while we report an elongation rate that is within the bounds of a bulk eukaryotic elongation rate of 3-10 amino acids per second as reported by previous studies, our results trend towards the lower end of the range which is unexpected for yeast-optimized constructs (Karpinets et al. 2006, Riba et al. 2019). We hypothesize that this may be due to nonideal conditions for yeast growth or protein expression during the duration of the assay. For example, it is unclear whether a proper level of aeration and mixing is achieved for yeast growth while within a 96-well plate. Growth conditions and protein expression may be impacted by improper aeration or through the presence of furimazine, the nanoluciferase substrate. Solving both these

issues would improve the reliability of our assay, especially when we consider expanding the scope to studying the impact of other regulatory factors and in other model organisms.

One of the major strengths of our elongation assay is the flexibility for use in studying other model organisms and factors that impact translation. Substitution of the yeast-optimized nanoluciferase reporter for other reporters opens the possibility of its use in different model organisms, such as in mammalian cells, allowing us to compare translation rates across organisms. Furthermore, we can quantify the impact of other factors known to affect translation including mRNA secondary structure, RNA binding proteins (RBPs), and cellular and environmental conditions. Highly structured mRNAs have been known to affect translation especially near the 5' end as the secondary structure must be unwound before ribosomes can proceed (Kozak 1989, Sagliocco et al. 1993, Babendure et al. 2006). However, an *in vitro* study by Mao and colleagues has found an opposite effect wherein protein expression is positively correlated with the strength of mRNA secondary structure (Mao et al. 2014). RNA binding proteins (RBPs) are critical players in the regulation of gene expression and recent advances in technology have allowed researchers to identify RBPs and their targets on a transcriptome-wide scale (Kishore et al. 2010, Hentze et al. 2018, Kapeli et al. 2017, Van Nostrand et al. 2016). However, much work remains to determine how each RBP influences gene expression of its targets and their associated mechanisms. Adaptation to changing environmental conditions such as stress is a widely conserved attribute across organisms and has long been known to impact gene expression and in particular, translation globally (Hockenberry et al. 2018, Yamasaki and Andersen 2008,

Dannfald et al. 2021, Eaglestone et al. 1999, Moore et al. 2016). Using variants of our elongation reporter assay, we can quantify the impact on gene expression of all these factors and begin to understand mechanisms that drive post-transcriptional regulation.

We have demonstrated that separate mechanisms are responsible for the negative impacts on protein expression, mRNA expression, and elongation rate between acute and distributed stalls. A recent preprint by Veltri and colleagues finds results consistent with ours, in which separate pathways are activated when comparing acute and distributed stalls (Veltri et al. 2021). Furthermore, they propose that cells are able to distinguish between these different types of stalls based on the orientation of the ribosomal subunits when stalled. While these findings represent an exciting development into translation surveillance and rescue pathways, a few open questions remain. First, can these two pathways be activated simultaneously on the same transcript and if so, are they contributing equally? Epistatic analysis and further molecular cloning to create constructs with varying combinations of stalls can allow us to determine how cells choose to respond to problematic transcripts. Second, what pathway do other types of stalling factors such as mRNA secondary structure activate and does it depend on spacing, ribosomal orientation, or other factors? From Veltri and colleagues, we find that the orientation of stalled ribosomes on transcripts may be a distinguishing factor for which pathway to activate. However, this does not exclude the possibility that other factors such as surveillance proteins or ribosome collision duration may be implicated. Third, what are the thresholds that the cell uses to distinguish between different types of stalls? For example, what distance between poor codons will

designate an acute versus a distributed stall? Answering these questions will allow us to further characterize the nuances of translation regulation.

In regards to the relationship between translation and mRNA localization during glucose starvation, we have found that Rvb1/2 is co-transcriptionally loaded onto stress-induced mRNAs which are destined for translational repression and localization to stress granules. One area of further study is to determine if the role of Rvb1/2 is conserved across different stressors such as oxidative stress, UV irradiation, amino acid starvation, and heat shock, all of which activate the integrated stress response pathway but through different signaling kinases (Pakos-Zebrucka et al. 2016). Furthermore, Rvb1/2 was identified as an enriched stress granule component in both yeast and mammalian stress granule proteomes, suggesting that the role of Rvb1/2 in glucose starvation in yeast may be conserved in mammalian systems but it is unclear if Rvb1/2 is conserved in other model organisms (Jain et al. 2016). Further study is required to understand the extent of Rvb1/2's role in post-transcriptional regulation and to discover other RBPs that are also co-transcriptionally loaded that have the potential to modulate gene expression.

Lastly, we have found a link between translatability and mRNA localization in which transcripts that undergo active translation remain diffuse and excluded from stress granules during glucose starvation and transcripts whose translation is repressed localize to stress granules. Tethering Rvb1/2 to a heat shock protein which is stress-induced and normally translationally active was sufficient to alter its localization and inhibit protein production. Further experiments are needed to confirm whether the opposite is true i.e. will a transcript that is normally translationally repressed be

excluded from stress granules if we force it to actively translate? These results will help build a model of how translation can be both regulated and be a regulator of gene expression. Together, these future topics of study contribute a more nuanced and well-understood view of the mechanisms behind post-transcriptional regulation.

4.2 Concluding Remarks

Post-transcriptional regulation represents an intricate coordination of RNA, RNA binding proteins, and other known and unknown factors in modulating gene expression. We have used *S. cerevisiae* as a model organism to study a few of the fundamental mechanisms in post-transcriptional regulation and in particular, the importance of translation in directing gene expression. We have developed a quantitative method to measure the impact of various cis and trans factors on elongation time and elucidate the relationship between elongation stalling and gene expression outcomes. We found that differences in the distribution of poor codons in a transcript are linked to different surveillance and rescue pathways. Additionally, we have studied the link between translation and mRNA localization during glucose starvation using fluorescence microscopy and have demonstrated that active translation is associated with exclusion from stress-associated mRNP granules. Furthermore, we uncovered a factor that is responsible for promoter-directed cytoplasmic fate for a certain class of stress-induced genes during glucose starvation. Taken together, these findings highlight the complexity and central role of translation as a process that is both regulated and regulates other processes in turn.

4.3 References

1. Babendure, J. R., Babendure, J. L., Ding, J. H., & Tsien, R. Y. (2006). Control of mammalian translation by mRNA structure near caps. *Rna*, *12*(5), 851-861.

2. Kozak, M. (1989). Circumstances and mechanisms of inhibition of translation by secondary structure in eucaryotic mRNAs. *Molecular and cellular biology*, *9*(11), 5134-5142.

3. Mao, Y., Liu, H., Liu, Y., & Tao, S. (2014). Deciphering the rules by which dynamics of mRNA secondary structure affect translation efficiency in Saccharomyces cerevisiae. *Nucleic acids research*, *42*(8), 4813-4822.

4. Sagliocco, F. A., Laso, M. V., Zhu, D., Tuite, M. F., McCarthy, J. E., & Brown, A. J. (1993). The influence of 5'-secondary structures upon ribosome binding to mRNA during translation in yeast. *Journal of Biological Chemistry*, *268*(35), 26522-26530.

5. Siomi, H., & Dreyfuss, G. (1997). RNA-binding proteins as regulators of gene expression. *Current opinion in genetics & development*, *7*(3), 345-353.

6. Kishore, S., Luber, S., & Zavolan, M. (2010). Deciphering the role of RNA-binding proteins in the post-transcriptional control of gene expression. *Briefings in functional genomics*, *9*(5-6), 391-404.

7. Hentze, M. W., Castello, A., Schwarzl, T., & Preiss, T. (2018). A brave new world of RNA-binding proteins. *Nature reviews Molecular cell biology*, *19*(5), 327-341.

8. Kapeli, K., Martinez, F. J., & Yeo, G. W. (2017). Genetic mutations in RNA-binding proteins and their roles in ALS. *Human genetics*, *136*(9), 1193-1214.

9. Van Nostrand, E. L., Pratt, G. A., Shishkin, A. A., Gelboin-Burkhart, C., Fang, M. Y., Sundararaman, B., Blue, S. M., Nguyen, T. B., Surka, C., Elkins, K., Stanton, R., Rigo, F., Guttman, M., & Yeo, G. W. (2016). Robust transcriptome-wide discovery of RNA-binding protein binding sites with enhanced CLIP (eCLIP). *Nature methods*, *13*(6), 508-514.

10. Hockenberry, A. J., Stern, A. J., Amaral, L. A., & Jewett, M. C. (2018). Diversity of translation initiation mechanisms across bacterial species is driven by environmental conditions and growth demands. *Molecular biology and evolution*, *35*(3), 582-592.

11. Yamasaki, S., & Anderson, P. (2008). Reprogramming mRNA translation during stress. *Current opinion in cell biology*, *20*(2), 222-226.

12. Dannfald, A., Favory, J. J., & Deragon, J. M. (2021). Variations in transfer and ribosomal RNA epitranscriptomic status can adapt eukaryote translation to changing physiological and environmental conditions. *RNA biology*, *18*(sup1), 4-18.

13. Eaglestone, S. S., Cox, B. S., & Tuite, M. F. (1999). Translation termination efficiency can be regulated in Saccharomyces cerevisiae by environmental stress through a prion-mediated mechanism. *The EMBO journal*, *18*(7), 1974-1981.

14. Moore, M., Gossmann, N., & Dietz, K. J. (2016). Redox regulation of cytosolic translation in plants. *Trends in plant science*, *21*(5), 388-397.

15. Veltri, A. J., D'Orazio, K. N., Lessen, L. N., Loll-Krippleber, R., Brown, G. W., & Green, R. (2021). Distinct ribosome states trigger diverse mRNA quality control pathways. *bioRxiv*.

16. Pakos-Zebrucka, K., Koryga, I., Mnich, K., Ljujic, M., Samali, A., & Gorman, A. M. (2016). The integrated stress response. *EMBO reports*, 17(10), 1374-1395.

17. Jain, S., Wheeler, J. R., Walters, R. W., Agrawal, A., Barsic, A., & Parker, R. (2016). ATPase-modulated stress granules contain a diverse proteome and substructure. *Cell*, 164(3), 487-498.